

# Reply to the interactive comment from the reviewers on “A biogenic CO<sub>2</sub> flux adjustment scheme for the mitigation of large-scale biases in global atmospheric CO<sub>2</sub> analyses and forecasts” by Agustí-Panareda et al.

## Reply to reviewer 1

We thank the reviewer for his/her comments. We have taken them into account in the revised manuscript to improve the motivation and the message of this work. In particular, we have highlighted the scientific content of our results. In the reply below we address all the reviewer’s concerns in order to clarify any misunderstanding on the importance of this study, and its relevance for the scientific community working on atmospheric composition and the carbon cycle. A pointer to the the different parts of the paper that have been modified is also provided in blue text for each general and specific comment addressed. The modifications performed in the revised paper are also highlighted in the latexdiff file provided.

### General comments

*\* In my opinion this paper has a number of problems and I believe that it is not currently suitable for publication in ACP. The first is that the paper contains relatively little scientific content, and there is nearly nothing that can be learned from the paper for a big audience. And even for researchers in the field of atmospheric CO<sub>2</sub> modeling, these methods are very system specific and not easily used by others even if they needed such flux adjustments. So this paper should probably remain a technical report for the Copernicus project, or perhaps it can be published in Geophysical Model Development journal. The case of why having better synoptic variations in forecast CO<sub>2</sub> is important is also not clearly made I think: who or what profits from this improved CO<sub>2</sub> forecast?*

The major aspects raised by the reviewer are addressed separately in detail below:

1. The scientific content of the paper.

Any atmospheric CO<sub>2</sub> forecast system requires a flux adjustment of some sort in order to constrain the budget of sources/sinks at the surface and avoid the growth of biases in the atmospheric background as documented by Agustí-Panareda et al. (2014). The scientific question addressed in this paper is how to use the best information we have in near-real time to adjust the fluxes in a way that reduces the bias of the atmospheric CO<sub>2</sub> forecast with the minimum deterioration of the synoptic skill. The simple flux adjustment scheme proposed here is based on a climatology of optimized fluxes and it could be applied

easily to other models. In the past other methods have been used by several modelling studies to remove biases attributed to the NEE fluxes. For instance, by globally re-scaling balanced NEE fluxes to match the residual land sink given by a climatology of TRANSCOM optimized fluxes (Nassar et al., 2010; Chen et al., 2013), or by re-scaling locally the NEE at boreal regions in order to get a better fit in the seasonal cycle (e.g. Messerschmidt et al. 2013, Keppel-Aleks et al. 2012).

This paper addresses the challenge of designing an online bias correction in a forecasting system with the aim to deliver an atmospheric CO<sub>2</sub> forecast and analysis that can be useful to the scientific community. The other methods mentioned previously are designed to work as a one-off correction and they offer less flexibility because they are performed offline. Tuning model parameters and/or re-scaling fluxes offline are not sufficient to guarantee a bias reduction in the system. An online adaptive system is required because errors in the meteorology can evolve as a result of regular operational Numerical Weather Prediction model upgrades and these affect the NEE budget in the model.

**An extract of the paragraphs above have been included in the methodology section.**

From the flux adjustment method presented in the manuscript we can learn several things about the model which can feedback later on model development as described in section 2.6 of the manuscript. The CAMS IFS model is just providing an example to show how this method can be applied efficiently in an operational forecasting system. It is also worth noting that the CAMS CO<sub>2</sub> forecast presented here is used by the scientific community for a variety of purposes (e.g. field experiments, boundary conditions). For this reason, we also think that the results, although specific to the CAMS CO<sub>2</sub> forecast model, could also be interesting to other scientists.

**An extract of the paragraph above has been included in the new Discussion subsection entitled “Aspects to be considered by users” as well as the summary section.**

2. The applicability of this method to other systems is straightforward.

The method could be useful for any model to be used in forecast mode and suffering from substantial biases in their land ecosystem flux budget. The use of the method can be two-fold: as a bias correction to the land ecosystem fluxes or as a diagnostic of bias contribution from different regions/vegetation types. The system is flexible and cheap to run. It only needs a few components: (i) A reference budget which can be obtained from a climatology of optimized fluxes (e.g. the MACC product can be easily obtained from [www-lscedods.cea.fr/invsat/PYVAR14\\_MACC/V2/Fluxes/3Hourly](http://www-lscedods.cea.fr/invsat/PYVAR14_MACC/V2/Fluxes/3Hourly) and it is well documented); (ii) Past 10-day NEE simulated by the forward model; (iii) The NEE anomaly of the forward model with respect to its climate based on a 10-year simulation. The use of the NEE anomaly is optional, and the benefits/drawbacks of using it are described in the revised version of the paper (see further explanation in the minor comments).

**An extract of the paragraph above has been included in the discussion section (first paragraph).**

3. Who or what profits from this improved CO<sub>2</sub> forecast?

The CO<sub>2</sub> forecast is a product freely available to the wide public and scientific community (<http://atmosphere.copernicus.eu>) with users from a variety of backgrounds. This

will be emphasized in the revised version of the manuscript, including the main scientific research areas that can benefit from a CO<sub>2</sub> forecast which are listed below:

- **Global data assimilation of atmospheric CO<sub>2</sub> observations**

The atmospheric CO<sub>2</sub> forecast is used as a prior to the atmospheric CO<sub>2</sub> analysis. For example, the CAMS atmospheric CO<sub>2</sub> analysis currently assimilates the GOSAT CO<sub>2</sub> product using a 4D-Var atmospheric data assimilation system (Massart et al. 2016). The reduction of the bias in the forecast by BFAS is highly desirable for data assimilation because the biases violate the assumption that the error distribution of the prior is centred around the true value.

The CO<sub>2</sub> analysis system could be used to assimilate/combine a wide range of observations in the future. Preliminary monitoring/intercomparison of different CO<sub>2</sub> satellite products can be easily performed to provide feedback to the scientific community working on satellite retrievals. The fact that the forecast can provide a realistic representation of the underlying atmospheric variability of CO<sub>2</sub> in a timely manner is an important part of this data assimilation and monitoring processes. One of the most prominent modes of variability in the current 5-day forecast is the day-to-day synoptic variability. Thus, the emphasis is on synoptic timescales.

- **CO<sub>2</sub> observing system**

The CO<sub>2</sub> forecast has been used in the research of bias corrections for satellite retrievals of OCO-2 lead by Chris O'Dell and could also be used in CH<sub>4</sub> satellite retrievals using the proxy method (Schepers et al. 2012). The predictive skill has also been used to support the planning of flight campaigns (e.g. CHARMEX, Ricaud et al. 2016, <http://charmex.lsce.ipsl.fr/>, and ACT-America, <http://www-air.larc.nasa.gov/missions/ACT-America/>) designed to improve our understanding of processes affecting atmospheric composition. It has also been used to demonstrate the use of new instruments in field experiments (e.g. Polarstern campaign, Klappenback et al. 2015). The detection of the atmospheric signals in the 1-day forecast (or nowcasting) can also help the interpretation of the observed variability from operational in situ networks (ICOS/InGOS monitoring), as well as expanding research networks (e.g. TCCON-RD) which aim to provide observations a few days behind real time.

- **CO<sub>2</sub> regional modelling**

Another core usage of the global forecast is as boundary conditions for regional models. In particular those studies focusing on city-scale resolution (e.g. Br  on et al. 2015, Boon et al. 2015) can benefit the most from the high resolution of the Numerical Weather Prediction (NWP) global model.

Because of all these growing needs for a CO<sub>2</sub> analysis/forecast in real time, there have been recent efforts to start similar analysis/forecasting systems by NASA GMAO ([http://acdb-ext.gsfc.nasa.gov/People/Colarco/Mission\\_Support/](http://acdb-ext.gsfc.nasa.gov/People/Colarco/Mission_Support/), Ott et al. 2015) and Environment Canada (Polavarapu et al. 2015) with their NWP models.

**The benefits of the improved forecast for the scientific community (data assimilation, CO<sub>2</sub> observing system, and CO<sub>2</sub> regional modelling) have been highlighted in the introduction and summary sections.**

\* *Another issue with the paper is the choice of the control run. Taking the fluxes from the neutral-biosphere in CTESSEL is clearly wrong, and there could have been many easy ways to improve on those. I think that a better benchmark is the available MACC fluxes, as the authors show that these already do quite a good job in matching observations if simply prescribed to the CAMS model. The authors state that these fluxes do not have synoptic variability, and I am not clear why this is because their resolution is never mentioned in the paper. But if diurnal and synoptic variations are needed, the simple method of Olsen and Randerson (2004) can be used to include the effect of temperature and light on monthly mean fluxes to get hourly ones. If the BAFS system was shown to be better than such an offline flux product, it would be much more clear to me that this way of BFAS is the way forward for CAMS.*

In the revised manuscript we have highlighted the benefits of using BFAS to correct the modelled NEE as part of the CTESSEL land-surface model instead of using an offline flux product, e.g. the climatology of the MACC optimized fluxes (used as benchmark in the paper). The MACC optimized fluxes have a resolution of 3 hours, but all night-time and day-time variations for time scales less than a week only come from the underlying prior fluxes. Using a 10-year climatology means that the synoptic variability of the fluxes is not present. Agustí-Panareda et al (2014) showed that the synoptic variability of the fluxes could be important when it comes to represent the synoptic atmospheric CO<sub>2</sub> variability in the boundary layer. The Olsen and Randerson (2004) method could be used to remediate part of this problem. However, this solution would not be as straightforward to apply in an online forecast as it is done in an offline mode, for which all the climate forcing parameters (2 m temperature and solar radiation can be retrieved beforehand). There are also other reasons for not using an offline NEE product or optimized fluxes directly in the CAMS CO<sub>2</sub> forecasting system:

- Downscaling the coarse optimized fluxes (2.5x3.75 degrees) at the resolution used by NWP models (currently 9 km at ECMWF) is not straightforward. Inconsistencies in the topography (particularly around mountains and coastlines) makes the low resolution fluxes difficult to use in a high resolution model.
- Coupling of CO<sub>2</sub> fluxes from terrestrial vegetation and the atmospheric model represents an important step towards a better understanding of the interaction between the ecosystem and regional atmospheric processes (Lu et al. 2001, Moreira et al, 2013). Boussetta et al. (2013) showed that the coupling between the CO<sub>2</sub> fluxes and the water and energy fluxes in the modelling of vegetation can improve the simulation of surface parameters such as temperature and humidity as well as NEE. This coupling has been shown to benefit the simulation of the CO<sub>2</sub> diurnal cycle in the atmospheric boundary layer in the tropics (Lu et al., 2005, Moreira et al. 2013).
- Finally, because offline NEE products or optimized fluxes are not available in near-real time, we would need to use a climatology. The inter-annual variability associated with the land sink cannot be considered when using just a climatology of NEE. Despite being a challenging aspect of the modelling, we think it is worth having inter-annual variability in the model forecast. The main rationale for this is based on the understanding that the climate variables simulated in the NWP model – such as temperature and precipitation – play an important role in explaining the inter-annual variability of NEE (Schaefer et al. 2002). The motivation for including the model inter-annual variability in the flux adjustment will be clarified in the revised manuscript.

**These three points above have been included in the Methodology section to explain the motivation behind the modelling of the CO<sub>2</sub> fluxes online.**

\* *It is not clear to me why certain metrics were chosen for evaluation. The authors present mean biases and standard deviations in Figures 9 and 10, correlation coefficients in Table 4, no metric for Figure 11, but there are never root-mean-square differences reported which I think are most useful. I think in figure 11 the MACC fluxes have the lowest RMSD than the BFAS fluxes. And from the captions it seems that both observations and simulations are done as daily (24-hour?) averages. I think that this daily averaging is needed because the independent adjustment of the GPP and TER scaling factors leads to strong variations in NEE that do not necessarily preserve a good diurnal cycle. But I might be wrong on that, as I could not assess this from the figures shown. 24-hour average observations could have a lot of hour-to-hour variability which should be shown by an error bar. The statistics and figures moreover seem to cover only the month of March and a few selected days in March. It remains unexplained why this choice was made, and what the metrics look like for other months. I would expect for instance in summer to see even larger day-to-day variations in NEE, and then also in atmospheric CO<sub>2</sub>*

Following the reviewer’s advice, we have computed the root-mean-square (RMS) error of the different CO<sub>2</sub> experiments with respect to observations at the tower sites shown in Fig 11 of the manuscript (see Table 1 below). With the RMS error it is not as easy to see the improvement in the modelled variability as with the correlation coefficient  $r$ , because the RMS error increases very rapidly when there is large variability. This effect can be clearly seen at Park Falls at 30 m above the surface. Despite the substantial improvement in the model variability with BFAS ( $r = 0.8$ ) compared to the CONTROL forecast ( $r = 0.3$ ), the RMS error is larger in BFAS than in the CONTROL experiment by more than 1 ppm. This happens because the BFAS experiment overestimates the amplitude of the synoptic variability which is nearly non-existent or even anticorrelated in the CONTROL experiment. At West Branch, the BFAS experiment has a much lower RMS error than both the experiments without BFAS and with optimized fluxes. Table 1 can be included in the supplement of the revised manuscript.

**The RMS error has been included in the evaluation of the flux adjustment results in the revised paper (see Table 1 and Figs. 3 and 5 in the Supplement.)**

The impact of BFAS on the diurnal cycle amplitude has been evaluated in the northern hemisphere land (north of 20°N) based hourly data from all the in situ stations compiled in the NOAA Obspack (2015) dataset for 2010 (Fig. 1 of this reply). The mean error of the diurnal cycle amplitude (daily max value minus daily min value) is reduced for all seasons, with larger improvements in winter, autumn and spring. The RMS error on the other hand is slightly worsened. This is not surprising since the reference optimized flux dataset is not designed to represent the synoptic variability of the diurnal cycle amplitude (see green and dark blue bars in Fig. 1 of this reply). Summer months have larger diurnal cycle amplitudes and as expected the model also has larger errors in JJA. However, the impact of BFAS on the RMS error is the same for all months.

**This assessment of the diurnal cycle has been included in the Supplement of the revised manuscript.**

\* *I would like to know what the added value is of having the gamma-parameter included in BFAS. The description of its calculation and adjustment is quite extensive but I do not really understand what role it plays. Perhaps there could be an experiment where BFAS is used without the adjustment in equation 3. After all, not needing the ensemble of forecasts would make the scheme a bit simpler, and perhaps just as good? I know I am likely to be wrong as the authors have decided to include this procedure in BFAS, but I would like to see the evidence to support*

Table 1: Root mean square error [ppm] of different forecast (FC) experiments with observations at three NOAA/ESRL tall towers for daily mean dry molar fraction of atmospheric CO<sub>2</sub> in March 2010. The dash symbol means the correlation is not significant.

NOAA/ESRL Tower site (ID)	Latitude, Longitude, Altitude	Sampling level [m]	BFAS FC	CTRL FC	OPT FC	OPT-CLIM FC
Park Falls, Wisconsin (LEF)	45.95°N, 90.27°W, 472 m	30 122 396	6.12 4.05 2.93	4.97 5.44 5.10	3.04 2.09 1.37	3.31 3.06 1.99
West Branch, Iowa (WBI)	41.72°N, 91.35°W, 242 m	31 99 379	3.79 2.91 2.46	10.39 9.94 8.91	5.06 2.95 3.20	6.96 3.92 2.43
Argyle, Maine (AMT)	45.03°N, 68.68°W, 50 m	12 30 107	3.72 3.55 2.86	3.76 3.36 3.37	2.35 1.66 1.06	1.30 0.82 0.76

that decision.

A new experiment has been performed in which the  $\gamma$  factor is set to zero in order to demonstrate the value of having the inter-annual variability in BFAS. Indeed the inter-annual variability can be important factor in the simulation of CO<sub>2</sub> (Schaefer et al. 2002, Chamard et al. 2003). However, because is not the same in every region/season/year it can also be difficult to demonstrate its impact with observations (Figs 2, 3, 4 and 5 of this reply). In BFAS, the use of the  $\gamma$  factor to represent the inter-annual variability from the model generally has a small impact. However, there are seasons and regions where we see the impact of using the  $\gamma$  factor. As expected, this impact tends to be larger in the tropics, where the model inter-annual variability is also largest (Agusti-Panareda et al. 2014). However, we can also see some impact in the northern and southern hemisphere for the MAM, JJA, SON seasons. In summary, including the inter-annual variability factor in BFAS is beneficial as in most cases it leads to a bias reduction, with just a few exceptions for the SON season (see LTrop in Fig. 4 and LN20N in Fig. 2 of this reply).

**The plots with the new experiment have been included in the Supplement. In addition, a summary of the experiment results has been included in the Methodology section 2.2 together with the rationale for including the inter-annual variability factor in the flux adjustment.**

## Minor comments

\* Page 3, line 5: I do not agree that the current monitoring of CO<sub>2</sub> relies on satellites and it is even a bit insulting to the real monitoring groups to say it. I suggest to change it because

*satellites do not yet see reliable CO<sub>2</sub>. In fact, the second part of this statement is also not right because the observations you show and that MACC fluxes rely on mostly come from flasks and not from in-situ instruments.*

The reference to in situ observations was meant to include both continuous and flask measurements (lines 8 to 10 in Page 3).

**In the revised version of the manuscript this has been clarified by specifying both explicitly.**

*\* Page 12, line 20: the current adjustment scheme for GPP and TER does not include any covariances between the adjustments, but we know that they often respond in the same direction and that errors are correlated. It would be good to think about an adjustment scheme that uses such information. Showing the posterior diurnal cycle is also needed.*

**This has been mentioned as future improvements planned for BFAS in section 6.3 of the revised manuscript. The impact on the diurnal cycle has been included in the supplement as mentioned above.**

*\* Page 13, line 20: You use now the names OPT-CLIM and later on in the text and tables CLIM-OPT. Is this the same run? It was to me confusing. Also see later remark about Table 2*

The runs are the same. **The text and Table 2 have been corrected in the revised version to use the consistent label for the OPT-CLIM experiment.**

*\* Page 14, line 20: A table listing the annual mean fluxes for transcom regions for all simulations would be valuable I think*

**The proposed table for the budget in the Transcom regions has been included in the Supplement of the revised manuscript.**

*\* Page 15, line 25: The SH problems could come from a different north to south transport characteristic of the two atmospheric models used (IFS and LMDZ?). Can this be illustrated with a simple SF6 simulation and compare it to observations?*

We think the negative bias in the southern hemisphere comes from biases in tropical Africa. Preliminary experiments to assimilate IASI CO<sub>2</sub> using the CO<sub>2</sub> forecast have shown a large systematic difference throughout the free tropospheric column over tropical Africa which is consistent with the negative bias in the southern hemisphere.

**This has been mentioned in the revised manuscript.**

*\* Acknowledgements: please check the data usage policy of NOAA as I do not believe you can simply take data from their FTP and then publish it with this statement.*

The authors have contacted Ed Dlugokencky regarding the acknowledgements and received his confirmation that these are sufficient. **An acknowledgement for the Obspack data used for the plots in the Supplement of the revised manuscript has been added.**

*\* Page 30, Table 2: I was confused because it says that CLIM-OPT uses MACC fluxes as reference in BFAS but from the methods I understood that CLIM-OPT or OPT-CLIM used the climatological fluxes from MACC directly as underlying biosphere fluxes? I discovered this only*



*towards the end of reading and it made me think I misunderstood the simulations completely. Even now I doubt it.*

CLIM-OPT uses the climatological fluxes from MACC (i.e. the total CO<sub>2</sub> flux) and BFAS just uses a climatology of the MACC residual biosphere fluxes.

**This has been clarified in Table 2 and in the text of the revised manuscript.**

*\* Figures 4 and 7: it would be better to use PgC/yr as units and not GtC/day because now they just look very small on the y-axis with many insignificant digits to start.*

If the units are changed to PgC/yr then the values have to be divided by 365, which result in even a larger number of insignificant decimal points. For this reason, the units have not been changed in the revised manuscript.

*\* I believe Figure 12 and 13 are not needed and could be removed.*

The authors disagree on this point. The fact that BFAS can change the gradient of the fluxes and as a result improve the atmospheric CO<sub>2</sub> synoptic variability is an achievement that needs to be properly documented.

## Reply to reviewer 2

### General comments

- This paper presents an enhancement to the CO<sub>2</sub> assimilation system used within the Copernicus tracer assimilation system at ECMWF. The enhancement is certainly useful and potentially quite important but it comes with its own problems. I believe these need to be discussed in the manuscript and addressed in how the new product is made available.*

We thank the reviewer for his insightful comments concerning the potential use of the CAMS CO<sub>2</sub> analysis product in flux inversion systems. The reply to each of the reviewer's points can be found below, together with a pointer to the section of the text that has been modified in the revised manuscripts (see blue text). A highlight of all the modification introduced in the revised manuscript can be found in the latexdiff file provided.

- The enhancement addresses the problem of large-scale biases in the fluxes which underlie the prior concentrations used in the assimilation. These biases are a serious matter since they mean that the probability densities assumed in the assimilation system (centered on the true value) don't, in fact, hold. So this is a potentially valuable improvement.*

This is a very important part of the motivation of this work because the atmospheric CO<sub>2</sub> forecast provides the prior information to the CAMS atmospheric CO<sub>2</sub> data assimilation. As the reviewer points out, the data assimilation system is only designed to reduce the random error, not the bias. Therefore, it is very important to bias correct the prior atmospheric mixing ratios from the forecast before assimilating any CO<sub>2</sub> observations. **We have included this point in the introduction of the revised manuscript to strengthen the motivation for BFAS.**



- *The problem arises when we consider what the generated CO<sub>2</sub> fields are used for. Although there is probably some benefit for improved retrievals of temperature and moisture by improving the CO<sub>2</sub> field the overwhelming use for the assimilated CO<sub>2</sub> products is in estimating surface fluxes. the statistical apparatus is identical to the assimilation of the CO<sub>2</sub> fields and the same restrictions apply. Among them is a firm prohibition on reusing information and the requirement that observations and prior are independent. Both of these are potentially violated in any downstream use of the BFAS product. Lets deal with these two problems in turn.*

The reviewer has an important point in that users of the CAMS CO<sub>2</sub> analysis/forecast products need to know what is the input data going into the product and what is the final uncertainty of the product. This is the case whether the users are working on flux inversion systems, planning of field experiments or using the product as boundary conditions for regional models.

Regarding the mixing of information in the analysis, this is currently not an issue for the CAMS CO<sub>2</sub> analysis system because the optimized fluxes used in BFAS are not based on satellite products; whereas the CAMS atmospheric CO<sub>2</sub> analysis is currently only assimilating satellite products.

For the users, we envisage that the atmospheric CO<sub>2</sub> analysis/forecast will be used as boundary conditions for regional flux inversion systems. In this case the possible correlated errors between such an analysis and the measurements assimilated by the inversion within the regional domain will likely be marginal, given all the processing that is involved between the inversion to estimate the MACC optimized fluxes, BFAS and the IFS 4D-Var used by the CAMS atmospheric CO<sub>2</sub> analysis. The possibility to infer the surface fluxes directly from the IFS CO<sub>2</sub> analysis would mean that some information from the observations assimilated by the MACC flux inversion system would already be present in the CAMS CO<sub>2</sub> analysis via BFAS. Thus, we have included information on the observations used in the flux inversion system to produce the optimised fluxes in the revised manuscript.

**Information on the uncertainty of the atmospheric CO<sub>2</sub> forecast with and without BFAS compared to the optimized flux experiments has been provided in terms of bias and root mean square error (RMSE) for different regions/seasons in the Supplement of the revised manuscript using barplots as shown in Figs 2, 3, 4 and 5 in this reply. All the issues relevant to users have been included in the Discussion as part of a new section entitled “Aspects to be considered by users”.**

- *I believe this paper is a potentially valuable contribution and look forward to the authors revision. If the authors accept my first point about the mixing of data into their CO<sub>2</sub> field then they also need to find a way of detailing which data was used to generate the flux fields that underlie BFAS.*

The flux fields underlying BFAS are primarily NEE modelled by the CTESSEL Carbon module in the IFS (Boussetta et al. 2013), which are then re-scaled using continental-scale climatological budgets from the MACC optimized fluxes of Chevallier et al. (2011, 2015). There is also some input from the EDGAR v4.2 anthropogenic emissions and the biomass burning emissions from GFAS (Kaiser et al. 2012). The information from these inventories is used to extract the NEE as a residual from the optimized fluxes.

**The documentation of the different data streams going into BFAS and their access (via the Copernicus Data Catalogue and the EDGAR database) has been included in the new Discussion subsection entitled “Aspects to be considered by users”.)**

## Specific comments

- *The assimilated CO<sub>2</sub> field now includes information from a prior informed by a previous flux inversion. This inversion presumably used measurements from the in situ network, aircraft and/or TCCON. We cant tell which without a detailed examination of the papers that underlie that inversion. We need to know because, if were going to use the BFAS product to drive a future inversion, we need to exclude those measurements. One might argue that the periods dont overlap but the evidence of the paper shows that the model-data mismatch is so strongly correlated from year to year (consistent seasonal errors in the pre-BFAS version) that this doesnt avoid the problem.*

**In the revised manuscript we have mentioned that since the BFAS product contains information from the optimized fluxes, users should be aware that the optimized fluxes assimilated most available background air-sample monitoring sites (listed in the supplement of Chevallier et al. 2015, see <http://www.atmos-chem-phys.net/15/11133/2015/acp-15-11133-2015-supplement.pdf> (see section 6.4 in the revised manuscript).**

Although we expect that observations ingested by the MACC inversion system of Chevallier et al (2011, 2015) will have an influence on the BFAS fluxes to some extent, we cannot quantify their degree of influence in this paper. We expect some information from the observations will be lost in the flux inversion process and specially in BFAS. The processing in BFAS involves spatial/temporal smoothing of the optimized fluxes over land with a 10-year averaging to construct the climatology and then the inclusion of the model interannual variability. The influence from these surface observations will be further diminished after the assimilation of satellite products in the analysis. In order to ensure independence between the CO<sub>2</sub> analysis and the background-air observations ingested by the MACC inversion system, the atmospheric CO<sub>2</sub> analysis could be sampled at non-background-air locations characterized by a large influence from the satellite products.

- *The second problem, of the prior estimate for a flux inversion being partially reflected in the data we use is not new with BFAS. It exists in the original Copernicus products too. Im unsure whether the mixing data and model information in the prior CO<sub>2</sub> field makes this problem worse but it seems like it should.*

The BFAS processing should bring the mean error and large-scale spatial distribution of the CTESSEL NEE fluxes closer to the MACC optimized fluxes. This probably implies that the BFAS fluxes will not be completely independent from the prior in the MACC flux inversion system. Thus, if the same prior would be used again to infer fluxes from the atmospheric CO<sub>2</sub> analysis data, then it would be likely that BFAS would make the problem associated with their lack of independence worse.

- *Finally there is the question of the uncertainty of the BFAS CO<sub>2</sub> field. There are two countervailing effects in play. First the bias correction of the prior has reduced residuals in the generated CO<sub>2</sub> field so that uncertainties (which are the statistics of the difference between estimated and true values) seem to have reduced. On the other hand an extra process has been added to the assimilation with a new set of parameters to scale prior fluxes. These will have their own uncertainty and should (since the posterior CO<sub>2</sub> field is sensitive to its prior) increase posterior uncertainty. Which of these wins out? I am always a little wary of criticizing a paper for things it did not do since no piece of research is complete. However its an important general rule that*

*products that are to be used as inputs to statistical procedures such as flux inversions need to specify their uncertainty as well as their mean.*

Plots showing characteristic biases and root mean square errors of the BFAS CO<sub>2</sub> field for different seasons/regions have been included in the supplement of manuscript (see Figures below) and referred to in the new section 6.4 entitled “Aspects to be considered by users”. These plots use all the observations from the NOAA Obstack (2015) dataset (excluding only the observations from CONTRAIL and HIPPO flights).

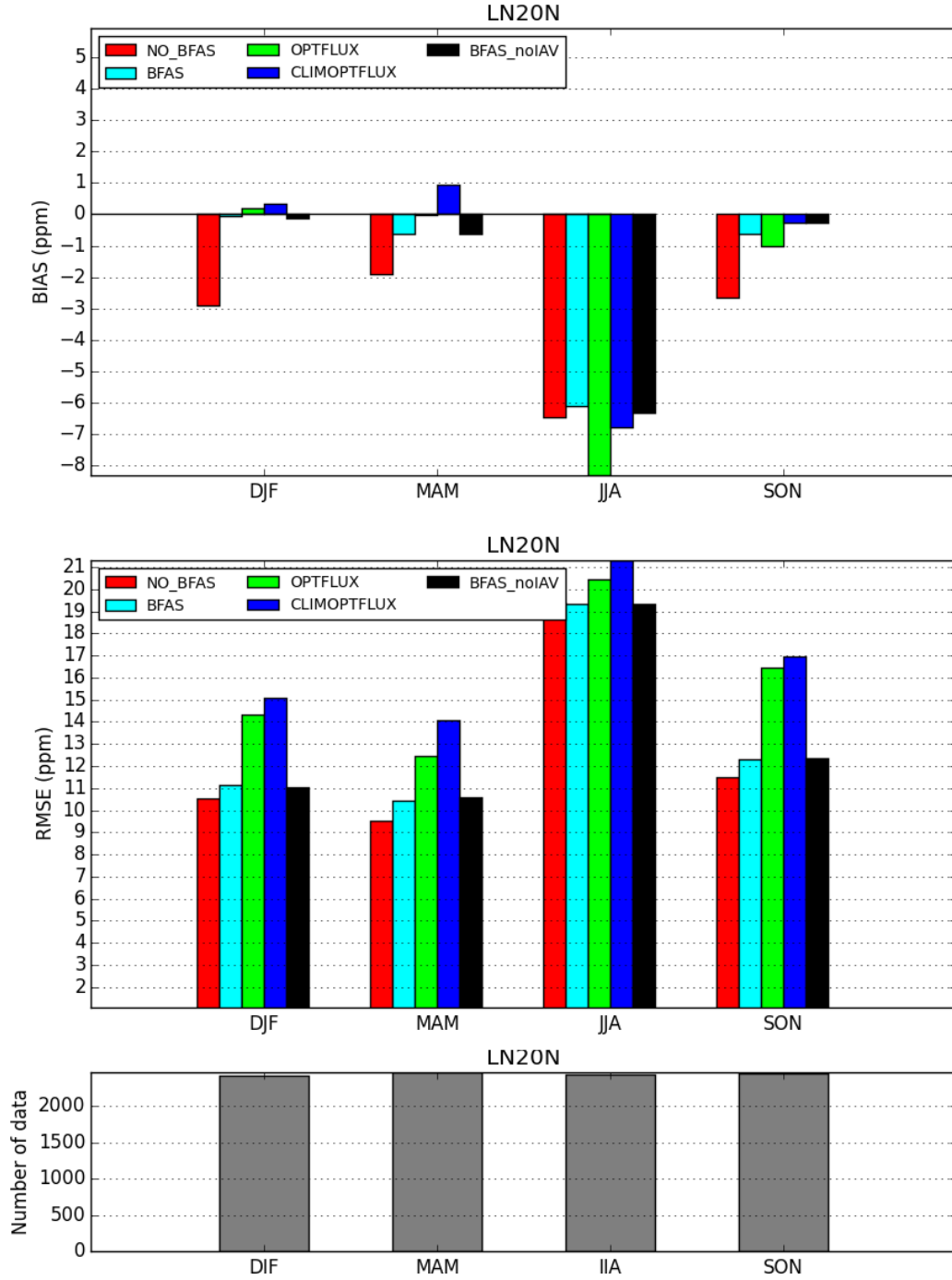


Figure 1: Evaluation of diurnal cycle amplitude of  $\text{CO}_2$  dry molar mixing ratio [ppm] for the different forecast experiments (see legend) in the northern hemisphere land (north of  $20^\circ\text{N}$ ) based on hourly data from all the in situ stations compiled in the NOAA Obspack (2015) dataset for 2010. Top panel: mean error; middle panel: root mean square error; and lower panel: number of observations.

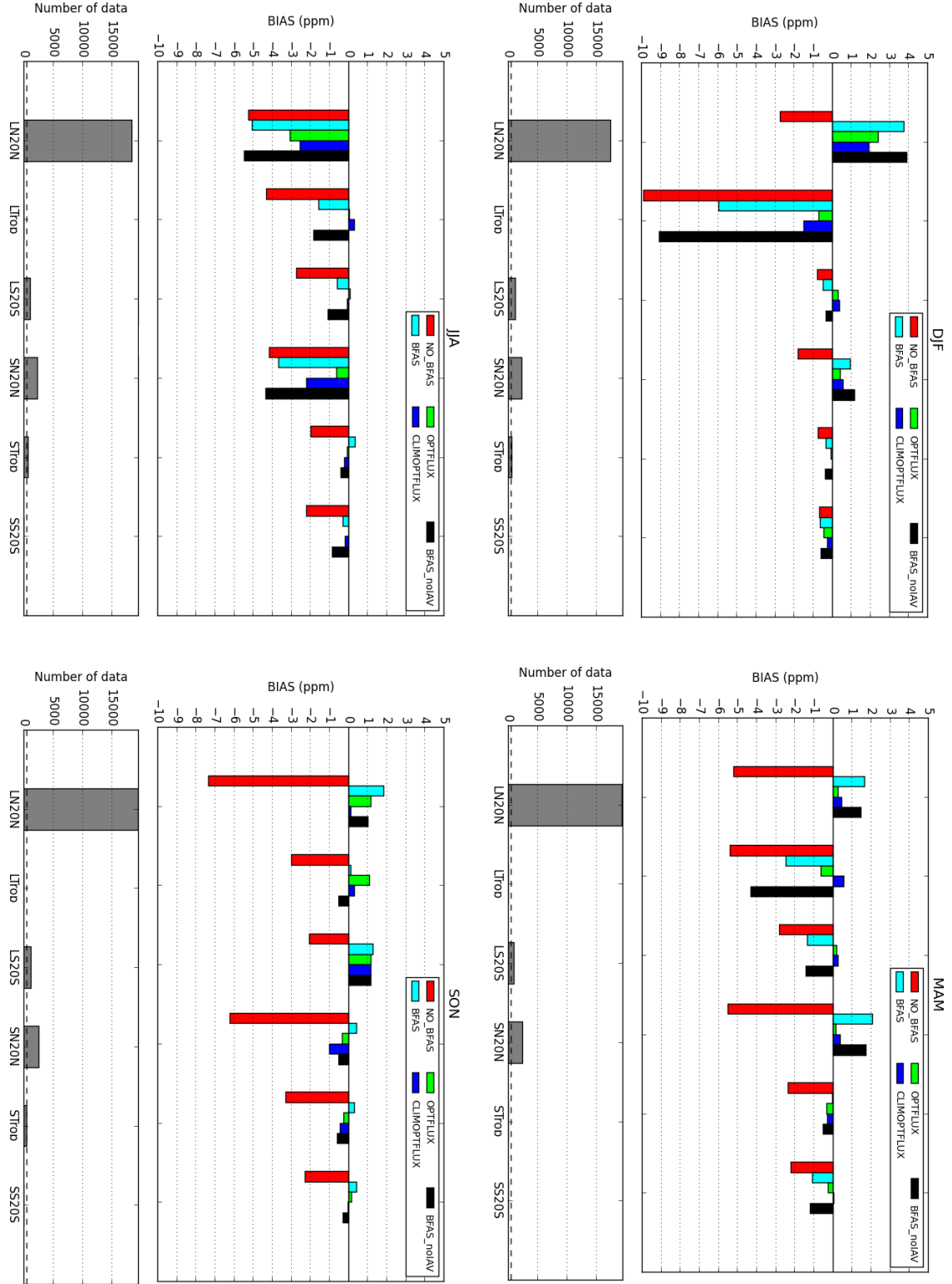


Figure 2: Mean error of atmospheric  $\text{CO}_2$  dry molar mixing ratio [ppm] for different forecast experiments (see legend) with respect to insitu and flask observations for different seasons and regions (N20N: north of  $20^\circ\text{N}$ ; Trop: between  $20^\circ\text{S}$  and  $20^\circ\text{N}$ ; S20S : south of  $20^\circ\text{S}$ ) with a separation between land and sea points denoted by a preceding “L” and “S” in the region name respectively. The observations were extracted from the NOAA Obspack (2015) dataset in 2010. The number of observations used for the statistics are shown as grey bars in the panel below each plot.

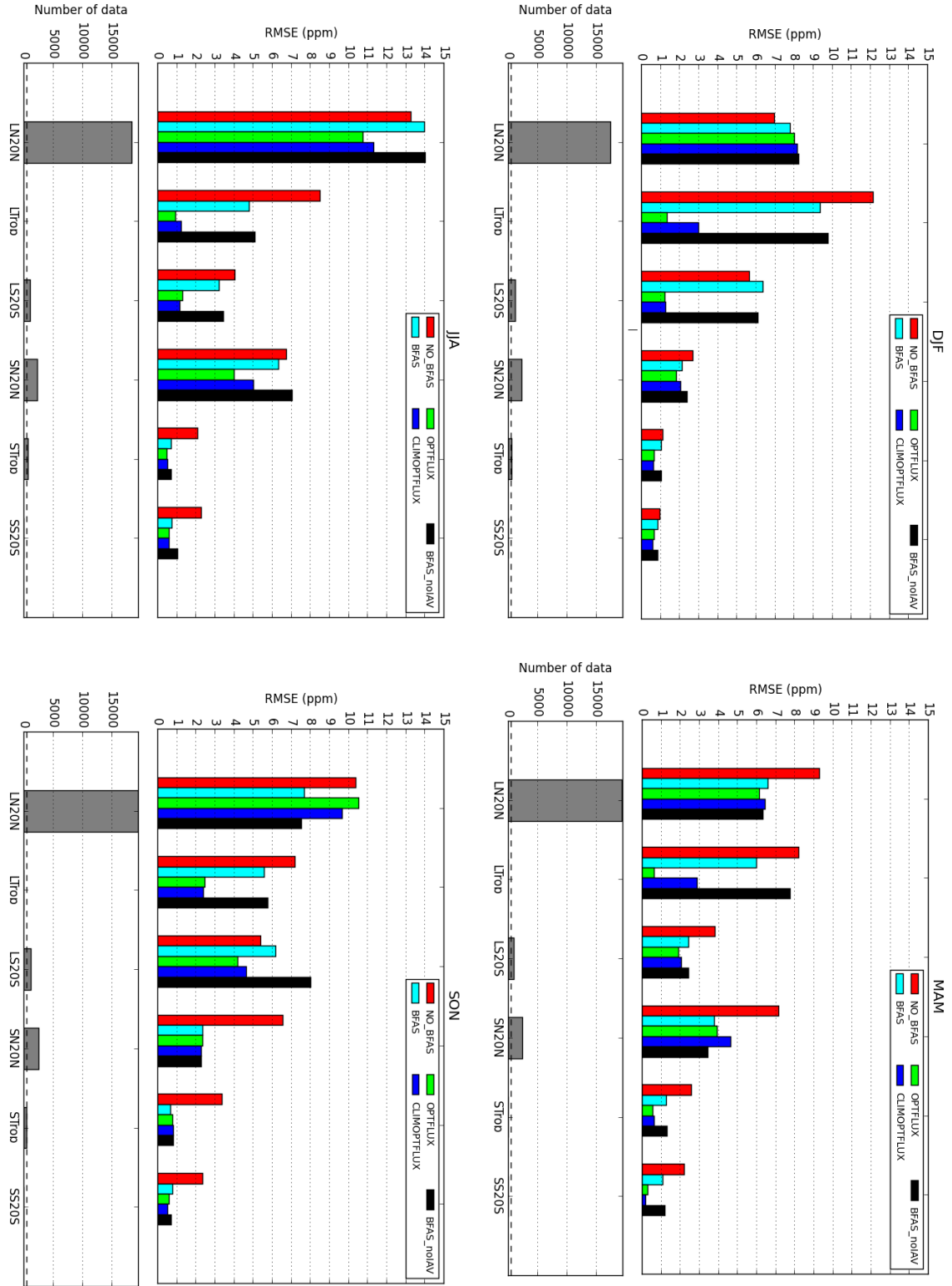


Figure 3: Root mean square error of atmospheric  $\text{CO}_2$  dry molar mixing ratio [ppm] for different experiments (see legend) with respect to insitu and flask observations for different seasons and regions as described in Fig. 2. The observations were extracted from the NOAA Obspack (2015) dataset in 2010. The number of observations used for the statistics are shown as grey bars in the panel below each plot.

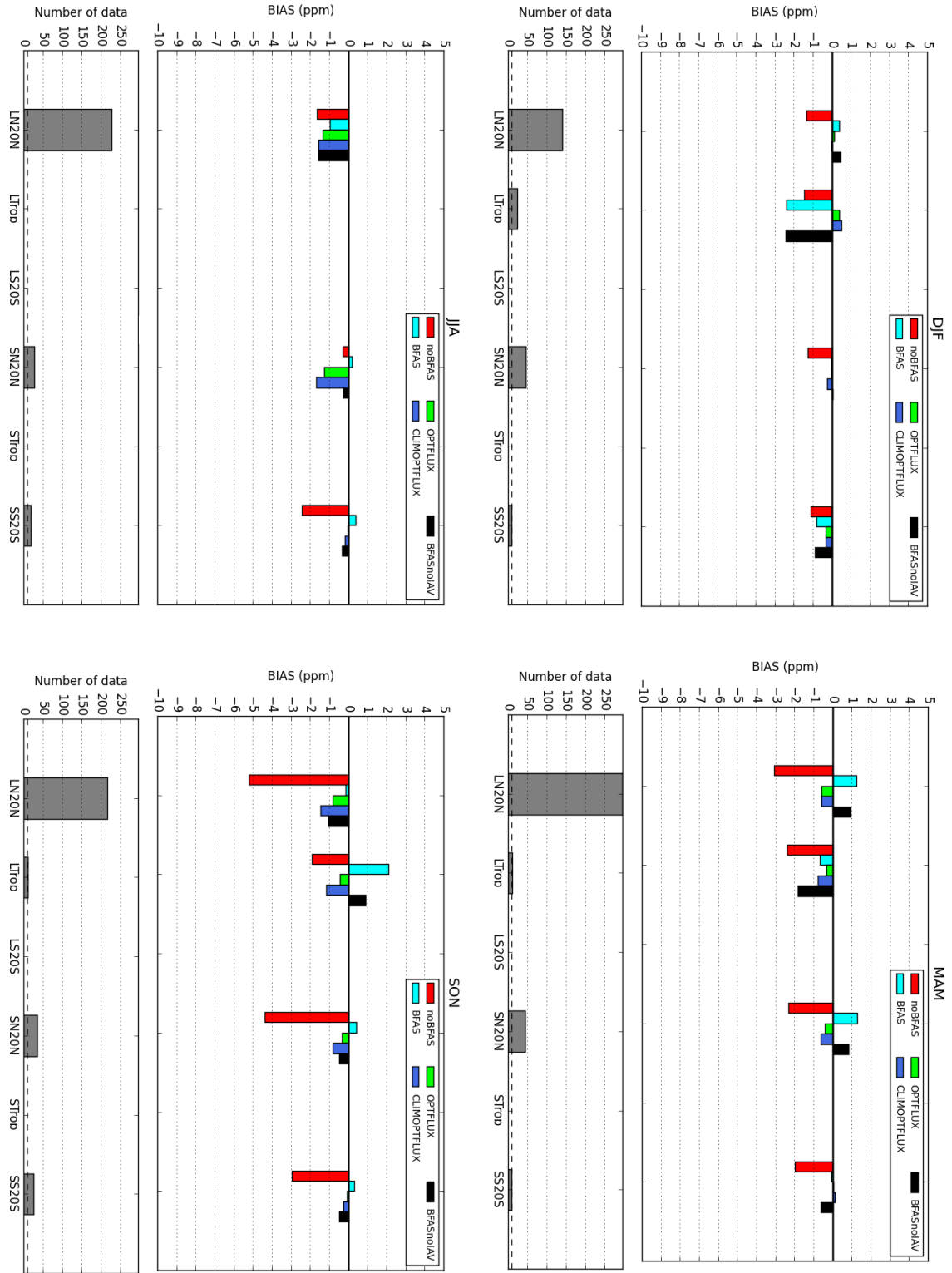


Figure 4: Mean error of atmospheric  $\text{CO}_2$  dry molar mixing ratio [ppm] for different experiments (see legend) with respect to NOAA aircraft vertical profiles (Sweeney et al. 2015) in the free troposphere (1000 m above surface) for different seasons and regions as described in Fig. 2. The observations were extracted from the NOAA Obspack (2015) dataset in 2010. The number of observations used for the statistics are shown as grey bars in the panel below each plot.



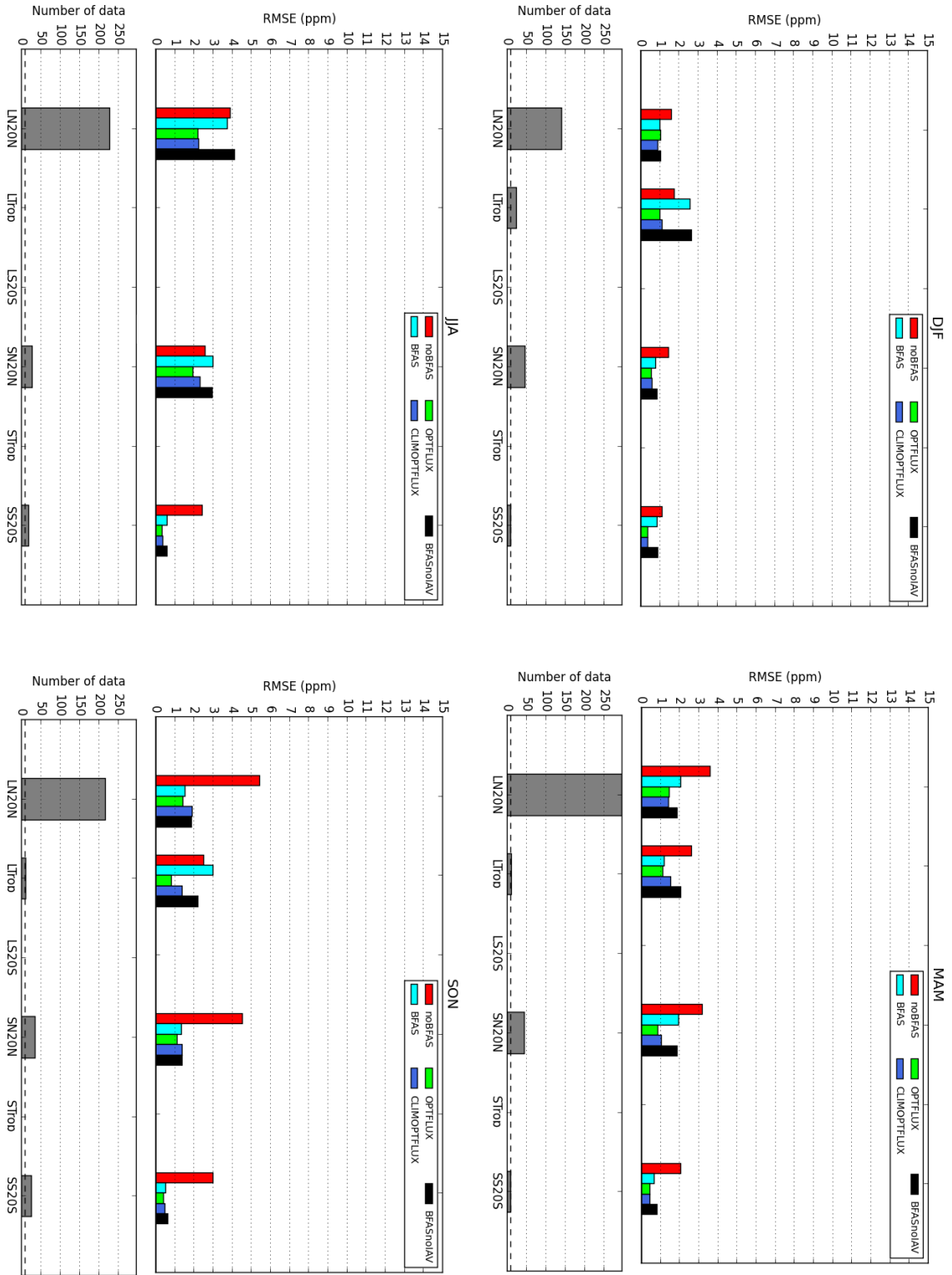


Figure 5: Root mean square error of atmospheric CO<sub>2</sub> dry molar mixing ratio [ppm] for different experiments (see legend) with respect to NOAA aircraft vertical profiles (Sweeney et al. 2015) in the free troposphere (1000 m above surface) for different seasons and regions as described in Fig. 2. The observations were extracted from the NOAA Obspack (2015) dataset in 2010. The number of observations used for the statistics are shown as grey bars.

## REFERENCES

- A. Agusti-Panareda, S. Massart, F. Chevallier and S. Boussetta, G. Balsamo, A. Beljaars and P. Ciais, N.M. Deutscher, R. Engelen and L. Jones, R. Kivi, J.-D. Paris, V.-H. Peuch and V. Sherlock, A.T. Vermeulen, P.O. Wennberg and D. Wunch: Forecasting global atmospheric CO<sub>2</sub>, *Atmospheric Chemistry and Physics*, 14, 11959–11983, doi:10.5194/acp-14-11959-2014, 2014.
- Boon, A. and Broquet, G. and Clifford, D. J. and Chevallier, F. and Butterfield, D. M. and Pison, I. and Ramonet, M. and Paris, J. D. and Ciais, P. (2015): TITLE = Analysis of the potential of near ground measurements of CO<sub>2</sub> and CH<sub>4</sub> in London, UK for the monitoring of city-scale emissions using an atmospheric transport model, *Atmospheric Chemistry and Physics Discussions*, 15, 33003–33048, doi:10.5194/acpd-15-33003-2015.
- Boussetta, S., Balsamo, G., Beljaars, A., Agusti-Panareda, A., Calvet, J.-C., Jacobs, C., van den Hurk, B., Viterbo, P., Lafont, S., Dutra, E., Jarlan, L., Balzarolo, M., Papale, D., and van der Werf, G. (2013) : Natural carbon dioxide exchanges in the ECMWF Integrated Forecasting System: implementation and offline validation, *J. Geophys. Res.-Atmos.*, 118, 1–24, doi: 10.1002/jgrd.50488.
- Bréon, F. M. and Broquet, G. and Puygrenier, V. and Chevallier, F. and Xueref-Remy, I. and Ramonet, M. and Dieudonné, E. and Lopez, M. and Schmidt, M. and Perrussel, O. and Ciais, P. (2015): An attempt at estimating Paris area CO<sub>2</sub> emissions from atmospheric concentration measurements, *Atmospheric Chemistry and Physics*, 15, 1707–1724, doi: 10.5194/acp-15-1707-2015.
- Chamard, P., F. Thiery, A. Di Sarra, L. Ciattaglia, L. De Silvestri, P. Grigioni, F. Monteleone and S. Piacentino (2003): Inter-Annual variability of atmospheric CO<sub>2</sub> in the Mediterranean: measurements at the island of Lampedusa. *Tellus B*, 55: 8393. doi: 10.1034/j.1600-0889.2003.00048.x.
- Chen, Z. H., Zhu, J. and Zeng, N. (2013): Improved simulation of regional CO<sub>2</sub> surface concentrations using GEOS-Chem and fluxes from VEGAS, *Atmospheric Chemistry and Physics*, 13, 7607–7618, 10.5194/acp-13-7607-2013.
- Chevallier F., N.M. Deutscher, T.J. Conway, P. Ciais, L. Ciattaglia, S. Dohe, M. Fröhlich, A.J. Gomez-Pelaez, D. Griffith, F. Hase, L. Haszpra, P. Krummel, E. Kyrö, C. Labuschne, R. Langenfelds, T. Machida, F. Maignan, H. Matsueda, I. Morino, J. Notholt, M. Ramonet, Y. Sawa, M. Schmidt, V. Sherlock, P. Steele, K. Strong, R. Sussmann, P. Wennberg, S. Wofsy, D. Worthy, D. Wunch, M. Zimnoch (2011): Global CO<sub>2</sub> fluxes inferred from surface air-sample measurements and from TCCON retrievals of the CO<sub>2</sub> total column, *Geophys. Res. Lett.*, 38, doi:10.1029/2011GL049899.
- Chevallier, F. (2015): On the statistical optimality of CO<sub>2</sub> atmospheric inversions assimilating CO<sub>2</sub> column retrievals, *Atmospheric Chemistry and Physics*, 15, 11133–11145, doi:10.5194/acp-15-11133-2015, <http://www.atmos-chem-phys.net/15/11133/2015/>.
- Kaiser, J.K., A. Heil, M.O. Andreae, A. Benedetti, N. Chubarova, L. Jones, J.-J. Morcrette, M. Razinger, M.G. Schultz, M. Suttie, G.R. van der Werf (2012): Biomass burning emissions estimated with a global fire assimilation system based on observed fire radiative power, *Biogeosci.*, 9, 527–554, doi:10.5194/bg-9-527-2012.
- Keppel-Aleks, G., P.O. Wennberg, R.A. Washenfelder and D. Wunch, T. Schneider, G.C. Toon

- , R.J. Andres and J.-F. Blavier , B. Connor , K.J. Davis , A.R. Desai and J. Messerschmidt , J. Notholt , C. M. Roehl , V. Sherlock , B.B. Stephens , S.A. Vay , S. C. Wofsy (2012): The imprint of surface fluxes and transport on variations in total column carbon dioxide, *Biogeosciences*, 9, 875–891, doi:10.5194/bg-9-875-2012.
- Klappenbach, F., Bertleff, M., Kostinek, J., Hase, F., Blumenstock, T., Agusti-Panareda, A., Razing, M., Butz, A. (2015): Accurate mobile remote sensing of XCO<sub>2</sub> and XCH<sub>4</sub> latitudinal transects from aboard a research vessel, *Atmospheric Measurement Techniques*, 8, 5023–5038, doi:10.5194/amt-8-5023-2015, 2015.
- Lu, L., A.S. Denning, M.A. da Silva Dias, P. Silva-Dias, M. Longo, S.R. Freitas, and S. Saatchi (2005): Mesoscale circulation and atmospheric CO<sub>2</sub> variation in the Tapajos Region, Para, Brazil. *Journal of Geophysical Research*, 110, D21102, doi:10.1029/2004JD005757.
- Lu, L., R.A. Pielke, Sr., G.E. Liston, W. Parton, D. Ojima, and M. Hartman (2001): The Implementation of a two-way Interactive Atmospheric and Ecological Model and its Application to the Central United States. *Journal of Climate*, 14, 900–919.
- Massart, S., Agustí-Panareda, A., Heymann, J., Buchwitz, M., Chevallier, F., Reuter, M., Hilker, M., Burrows, J. P., Deutscher, N. M., Feist, D. G., Hase, F., Sussmann, R., Desmet, F., Dubey, M. K., Griffith, D. W. T., Kivi, R., Petri, C., Schneider, M., Velasco, V. A. (2016): Ability of the 4-D-Var analysis of the GOSAT BESD XCO<sub>2</sub> retrievals to characterize atmospheric CO<sub>2</sub> at large and synoptic scales, *Atmospheric Chemistry and Physics*, 16, 1653–1671, doi:10.5194/acp-16-1653-2016.
- Messerschmidt, J., N. Parazoo, D. Wunch, N.M. Deutscher, C. Roehl, T. Warneke and P.O. Wennberg (2013): Evaluation of seasonal atmosphere-biosphere exchange estimations with TCCON measurements, *Atmospheric Chemistry and Physics*, 13 , 5103–5115, doi:10.5194/acp-13-5103-2013.
- Moreira, D. S., Freitas, S. R., Bonatti, J. P., Mercado, L. M., Rosário, N. M. É., Longo, K. M., Miller, J. B., Gloor, M., Gatti, L. V. (2013): Coupling between the JULES land-surface scheme and the CCATT-BRAMS atmospheric chemistry model (JULES-CCATT-BRAMS1.0): applications to numerical weather forecasting and the CO<sub>2</sub> budget in South America, *Geoscientific Model Development*, 6, 1243–1259, doi:10.5194/gmd-6-1243-2013.
- Nassar, R., Jones, D. B. A., Suntharalingam, P., Chen, J. M., Andres, R. J., Wecht, K. J., Yantosca, R. M., Kulawik, S. S., Bowman, K. W., Worden, J. R., Machida, T., Matsueda, H. (2010): Modeling global atmospheric CO<sub>2</sub> with improved emission inventories and CO<sub>2</sub> production from the oxidation of other carbon species, *Geosci. Model Dev.*, 3, 689716, doi:10.5194/gmd-3-689-2010.
- NOAA Obspack (2015): Cooperative Global Atmospheric Data Integration Project; Multi-laboratory compilation of atmospheric carbon dioxide data for the period 1968–2014; `obspace_co2_1_GLOBALVIEWplus_v1.0.2015-07-30`; NOAA Earth System Research Laboratory, Global Monitoring Division. doi: 10.15138/G3RP42, <http://dx.doi.org/10.15138/G3RP42>
- Olsen, S.C. and Randerson, J.T. (2004): Differences between surface and column atmospheric CO<sub>2</sub> and implications for carbon cycle research, *Journal of Geophysical Research*, 109, D02301, doi:10.1029/2003JD003968.
- Polavarapu, S.M., M. Neish, M. Tanguay, C. Girard, J. de Grandpré, S. Gravel, K. Semeniuk, and D. Chan (2015): Adapting a weather forecast model for greenhouse gas simulation, *AGU Fall Meeting*, San Francisco, 15–18 December 2015, Poster A31B-0037.

P. Ricaud, R. Zbinden, V. Catoire, V. Brocchi, F. Dulac, E. Hamonou, J.-C. Canonici, L. El Amraoui, S. Massart, B. Piguet, U. Dayan, P. Nabat, J. Sciare, M. Ramonet, M. Delmotte, A. G. di Sarra, D. Sferlazzo, T. Di Iorio, S. Piacentino, P. Cristofanelli, N. Mihalopoulos, G. Kouvarakis, S. Kleanthous, M. Pikridas, C. Savvides, R. E. Mamouri, A. Nisantzi, D. G. Hadjimitsis, J.-L. Atti, H. Ferr, P. Theron, Y. Kangah, N. Jaidan, P. Jacquet, S. Chevrier, C. Robert, A. Bourdon, J.-F. Bourdinot, and J.-C. Etienne (2016): Overview of the Gradient in Longitude of Atmospheric constituents above the Mediterranean basin (GLAM) airborne summer campaign (submitted to ACP).

MS No.: acp-2016-295 MS Type: Research article Iteration: Initial Submission Special Issue: CHemistry and AeRosols Mediterranean EXperiments (ChArMEx) (ACP/AMT inter-journal SI)

Schaefer, K., A.S. Denning, N. Suits, J.Kaduk, I. Baker, S. Los, L. Prihodko (2002): Effect of climate on inter-annual variability of terrestrial CO<sub>2</sub> fluxes, *Global Biogeochemical Cycles*, 16.

Schepers, D, S. Guerlet, A. Butz and J.Landgraf, C. Frankenberg, O. Hasekamp and J.-F. Blavier, N.M. Deutscher, D.W.T. Griffith , F. Hase, E. Kyro, I. Morino and V. Sherlock, R. Sussmann, I. Aben (2012): Methane retrievals from Greenhouse Gases Observing Satellite (GOSAT) shortwave infrared measurements: Performance comparison of proxy and physics retrieval algorithms, *Journal of Geophysical Research*, 117, D10307, doi:10.1029/2012JD017549.

Sweeney, C., A. Karion, S. Wolter, T. Newberger, D. Guenther, J. A. Higgs, A. E. Andrews, P. M. Lang, D. Neff, E. Dlugokencky, J. B. Miller, S. A. Montzka, B. R. Miller, K. A. Masarie, S. C. Biraud, P. C. Novelli, M. Crotwell, A. M. Crotwell, K. Thoning, and P. P. Tans (2015): Seasonal climatology of CO<sub>2</sub> across North America from aircraft measurements in the NOAA/ESRL Global Greenhouse Gas Reference Network, *Journal of Geophysical Research: Atmospheres*, 120, 10, doi:10.1002/2014JD022591.

# A biogenic CO<sub>2</sub> flux adjustment scheme for the mitigation of large-scale biases in global atmospheric CO<sub>2</sub> analyses and forecasts

A. Agustí-Panareda<sup>1</sup>, S. Massart<sup>1</sup>, F. Chevallier<sup>2</sup>, G. Balsamo<sup>1</sup>, S. Boussetta<sup>1</sup>, E. Dutra<sup>1</sup>, and A. Beljaars<sup>1</sup>

<sup>1</sup>European Centre for Medium-Range Weather Forecasts, Reading, UK

<sup>2</sup>Laboratoire des Sciences du Climat et l'Environnement, Gif-sur-Yvette, France

Correspondence to: A. Agustí-Panareda (anna.agusti-panareda@ecmwf.int)

**Abstract.** Forecasting atmospheric CO<sub>2</sub> daily at the global scale with a good accuracy like it is done for the weather is a challenging task. However, it is also one of the key areas of development to bridge the gaps between weather, air quality and climate models. The challenge stems from the fact that atmospheric CO<sub>2</sub> is largely controlled by the CO<sub>2</sub> fluxes at the surface, which are difficult to constrain with observations. In particular, the biogenic fluxes simulated by land surface models show skill in detecting synoptic and regional-scale disturbances up to sub-seasonal time-scales, but they are subject to large seasonal and annual budget errors at global scale, usually requiring a posteriori calibration. This paper presents a scheme to diagnose and mitigate model errors associated with biogenic fluxes within an atmospheric CO<sub>2</sub> forecasting system. The scheme is an adaptive calibration referred to as Biogenic Flux Adjustment Scheme (BFAS) and it can be applied automatically in real time throughout the forecast. The BFAS method generally improves the continental budget of CO<sub>2</sub> fluxes in the model by combining information from three sources: (1) retrospective fluxes estimated by a global flux inversion system, (2) land-use information, (3) simulated fluxes from the model. The method is shown to produce enhanced skill in the daily CO<sub>2</sub> 10-day forecasts without requiring continuous manual intervention. Therefore, it is particularly suitable for near-real-time CO<sub>2</sub> analysis and forecasting systems.

European Union Copernicus Atmosphere Monitoring Service (CAMS). CAMS uses the Numerical Weather Prediction (NWP) Integrated Forecasting system (~~HFS~~for Composition (C-IFS)) of the European Centre for Medium range Weather Forecasts (ECMWF) to produce near-real-time global atmospheric composition analysis and forecasts, including CO<sub>2</sub> (Agustí-Panareda et al., 2014) along with other environmental and climate relevant tracers (Flemming et al., 2009; Morcrette et al., 2009; Massart et al., 2014). The purpose of the real-time CO<sub>2</sub> analysis/forecasting system is to provide timely products that can be used by the scientific community among other users. For example, those working on new instruments, field experiments, satellite retrieval products, regional models requiring boundary conditions, or planning flight campaigns.

The present monitoring of global atmospheric CO<sub>2</sub> relies on observations of atmospheric CO<sub>2</sub> from satellites – e.g. Greenhouse Gases Observing Satellite (GOSAT, [www.gosat.nies.go.jp](http://www.gosat.nies.go.jp)); Orbiting Carbon Observatory 2 (OCO-2, [oco.jpl.nasa.gov](http://oco.jpl.nasa.gov)) – and flask and in situ networks – e.g. National Oceanic and Atmospheric Administration Earth System Research Laboratory (NOAA/ESRL, [www.esrl.noaa.gov/gmd](http://www.esrl.noaa.gov/gmd)); Integrated Carbon Observation System (ICOS, [icos-atc.lscce.ipsl.fr](http://icos-atc.lscce.ipsl.fr)); Environment Canada ([www.ec.gc.ca/mges-ghgm](http://www.ec.gc.ca/mges-ghgm)) – which are assimilated by global tracer transport models to infer changes in atmospheric CO<sub>2</sub> (~~e.g. ?~~) (e.g. Massart et al., 2015) or by flux inversion systems (e.g. Peylin et al., 2013) to estimate the large-scale surface fluxes of CO<sub>2</sub>.

The current ~~CAMS-C-IFS~~ CO<sub>2</sub> analysis is produced by assimilating CO<sub>2</sub> data retrieved from GOSAT by the University of Bremen (Heymann et al., 2015), as well as all the meteorological data that is routinely assimilated in the operational meteorological analysis at ECMWF. ?-Massart et al. (2015) have shown that the atmospheric data

## 1 Introduction

Earth-observing strategies focusing on carbon cycle systematic monitoring from satellites, flask and in situ networks (Ciais et al., 2014; Denning et al., 2005) are leading to an increasing number of near-real-time observations available to systems such as those developed in the framework of the

assimilation system alone cannot completely remove the biases in the background atmospheric CO<sub>2</sub> associated with the accumulation of errors in the CO<sub>2</sub> fluxes from the model. This happens because currently the CO<sub>2</sub> surface fluxes in the IFS data assimilation system cannot be constrained by observations. The model biases in atmospheric CO<sub>2</sub> also present a problem for the data assimilation system because its optimisation relies on the assumption that both model and observations are unbiased. It is therefore imperative to remove any large biases before assimilating observations. In this paper, we present a method to reduce the atmospheric CO<sub>2</sub> model biases by adjusting the CO<sub>2</sub> surface fluxes in a near-real-time CO<sub>2</sub> analysis/forecasting system, such as the one used by CAMS C-IFS at ECMWF.

Many different methods already exist to adjust CO<sub>2</sub> fluxes by using observations of atmospheric CO<sub>2</sub> within flux inversion systems (Rödenbeck et al., 2003; Gurney et al., 2003; Peters et al., 2007). However, these are not all suitable for the CAMS C-IFS real-time monitoring system. Flux inversion systems adjust the fluxes by either inferring the model parameters in Carbon Cycle Data Assimilation Systems also known as CCDAS (Rayner et al., 2005; Scholze et al., 2007; Rayner et al., 2011), or the fluxes themselves (Houweling et al., 2015). CCDAS has the advantage of working in prognostic mode once the model parameters have been optimised. Nevertheless, it can also be prone to aliasing information to the wrong model parameter when the processes that contribute to the variability of atmospheric CO<sub>2</sub> are not properly represented in the model or missing altogether. Estimating directly the CO<sub>2</sub> fluxes does not rely on the accurate representation of complex/unknown processes in the CO<sub>2</sub> flux model, but the resulting optimised fluxes do not have predictive skill. Both approaches generally use long data assimilation windows of several weeks to years in order to be able to constrain the global mass of CO<sub>2</sub> by relying mainly on high quality in situ flask and continuous observations which are relatively sparse in time and space. This general requirement for long assimilation windows is incompatible with the current NWP framework (e.g. a 12-h window is currently used in the IFS). In addition to that, the CO<sub>2</sub> observations from flask and most in situ stations used by these flux inversion systems are not available in near-real time.

Considering all the aspects mentioned above, a Biogenic Flux Adjustment Scheme (hereafter called BFAS) suitable for the NWP framework is proposed which aims to combine the best characteristics of both flux inversion approaches. Namely, the mass constraint from the optimised fluxes is used to correct the biases of the modelled CO<sub>2</sub> fluxes while keeping the predictive skill of the modelled fluxes at synoptic scales. The main objective of BFAS is to reduce the large-scale biases of the background atmospheric CO<sub>2</sub>. This should improve the representation of the atmospheric CO<sub>2</sub> large-scale gradients, and thereby also lead to a better forecast of atmospheric CO<sub>2</sub> synoptic variability.

The details of the flux adjustment scheme are provided in Sect. 2. Section 3 describes the IFS experiments done to test the impact of BFAS on the atmospheric CO<sub>2</sub> forecast. From the experiments, different aspects of the flux adjustment can be monitored (i.e. the scaling factors and the resulting budget) as shown in Sect. 4. The resulting atmospheric CO<sub>2</sub> forecast fit to observations after applying BFAS is presented in Sect. 5. The potential use of BFAS for model development and the possibility of including BFAS in the data assimilation system are discussed in Sect. 6. Finally, Sect. 7 gives a summary of the flux adjustment achievements and possible developments for the future.

## 2 Methodology

~~The flux adjustment scheme aims at reducing the large-scale biases in the background atmospheric CO<sub>2</sub> of the current CAMS forecasting system.~~ Any atmospheric CO<sub>2</sub> analysis/forecast system requires a flux adjustment of some sort in order to constrain the budget of sources/sinks at the surface and avoid the growth of mean errors in the atmospheric background (Agustí-Panareda et al., 2014). The scientific question addressed in this paper is how to use the best information we have in near-real time to adjust the fluxes in a way that reduces the bias of the atmospheric CO<sub>2</sub> in the model with the minimum deterioration of the synoptic skill to predict day-to-day variability.

Agustí-Panareda et al. (2014) documented the configuration of the CO<sub>2</sub> forecasting system and showed that the large biases in atmospheric CO<sub>2</sub> are consistent with errors associated with the budget of CO<sub>2</sub> surface fluxes, in particular the Net Ecosystem Exchange (NEE) modelled by the CTESSEL carbon model (Boussetta et al., 2013) within the C-IFS.

There are three main reasons for modelling NEE fluxes online as opposed to using offline fluxes such as optimized fluxes from flux inversion systems directly in the model: (i) the coupling of CO<sub>2</sub> biogenic fluxes with the atmospheric model can lead to improvements in both the understanding of interactions between ecosystems and the evolution of CO<sub>2</sub> in the atmospheric boundary layer (Lu et al., 2001; Moreira et al., 2013) and the forecast skill of energy and water cycle fluxes in NWP models (Boussetta et al., 2013); (ii) the use of offline fluxes would entail a loss of information and the introduction of topographical inconsistencies when downscaling fluxes from low resolution (e.g. typically a few degrees in optimized fluxes) to high resolution (e.g. currently 9 km in ECMWF NWP model); (iii) the non-availability of these offline fluxes in near-real time implies the interannual variability of the NEE fluxes (Schaefer et al., 2002) cannot be represented.

The challenge remains of how to reduce the large-scale biases associated with the modelled fluxes in real time. Because these biogenic fluxes are modelled online, a one-off scaling of the fluxes



using a climatology of the annual global budget (Nassar et al., 2010; Chen et al., 2013) or re-scaling locally the NEE in order to get a better fit with the seasonal cycle (Messerschmidt et al., 2013; Keppel-Aleks et al., 2012) are not suitable methods, as we do not know the annual budget of the model in real-time.

Optimised fluxes from flux inversion systems constitute the best available estimate of the CO<sub>2</sub> fluxes given the observed variations of CO<sub>2</sub> in the atmosphere at global scales. Thus, they can provide a reference benchmark for the modelled fluxes. The large-scale biases in the CO<sub>2</sub> fluxes can be diagnosed by computing the budget (i.e. integrated) differences between modelled fluxes and optimised fluxes over continental and supra-synoptic spatial and temporal scales ( $\geq 1000$  km, 10 days). Working with budgets over scales beyond the synoptic scale allows the detection of large-scale biases without interfering with the synoptic skill of the model.

It is important to note that there are uncertainties and limitations that should be considered when using optimised fluxes. Optimised fluxes are computed with flux inversion systems at low resolutions ( $\sim$  hundreds of km) compared to the NWP resolution used for the CO<sub>2</sub> forecasts ( $\sim$  tens of km), and they are most reliable at continental and supra-synoptic scales. Moreover, they have the limitation of not being available in near-real time, unlike the meteorological observations or CO<sub>2</sub> satellite retrievals (Massart et al., 2015). Because of that, a climatology of the optimised fluxes has to be used as a reference.

Finally, optimised fluxes only provide information on the total CO<sub>2</sub> flux because flux inversion systems are not able to attribute the CO<sub>2</sub> variability to the different processes controlling the fluxes, such as vegetation, anthropogenic sources and fires.

The CO<sub>2</sub> forecast evaluation by Agustí-Panareda et al. (2014) showed that the Net Ecosystem Exchange (NEE) modelled by the CTESSEL carbon model (Boussetta et al., 2013) within the IFS is the main responsible for the large global biases in the atmospheric CO<sub>2</sub> seasonal cycle. Generally, from all these fluxes, the land CO<sub>2</sub> fluxes from vegetation and soils in models are associated with high uncertainty (Le Quéré et al., 2015). For this reason, the Global Carbon Project provides the CO<sub>2</sub> budget from land vegetation – also known as the land sink – as a residual to close the carbon budget (see [www.globalcarbonproject.org/carbonbudget](http://www.globalcarbonproject.org/carbonbudget)). Following the land sink residual approach, the optimised NEE can be computed as the residual of optimised fluxes by subtracting the other prescribed fluxes. A set of 10-day mean budgets of this residual NEE from optimised fluxes is then computed daily for different regions and vegetation types over a period of 10 years to build the NEE climatology that can be used as a reference. In order to account for the inter-annual variability of NEE, the reference climatology is also adjusted with an inter-annual variability factor obtained from the model.

The flux adjustment scheme essentially estimates the bias of the modelled NEE budget with respect to the reference NEE budget for each region and vegetation type as a scaling factor  $\alpha$ :

$$\alpha = \frac{f^O}{f^M} \quad (1)$$

where  $f$  is the 10-day mean NEE budget computed daily over a specific vegetation type and region,  $f^O$  is the reference budget based on the MACC-13R1 optimised fluxes (Chevallier et al., 2010), and  $f^M$  is the budget of the modelled fluxes. Figure 1 shows how the BFAS scheme interacts with the model to produce the flux-corrected atmospheric CO<sub>2</sub> forecast. First of all, the uncorrected NEE fluxes from the model are retrieved. Then their budget is compared with the budget of the NEE climatology from the optimised fluxes adjusted with the NEE anomaly from the model. The scheme produces maps with scaling factors of the biogenic fluxes before the forecast run. Subsequently, these maps are then used to scale the forecast of NEE. There are three major building blocks required for the computation of these scaling factors:

- The computation of the NEE budget using temporal and spatial aggregation criteria (e.g. 10 days, vegetation types, different regions).
- A reference NEE dataset used to diagnose the model biases (e.g. optimised fluxes from global flux inversion systems such as the MACC-13R1 dataset from Chevallier et al. (2010)).
- The partition of the NEE adjustment into the two modelled ecosystem fluxes that make up the NEE flux: i.e. Gross Primary Production (GPP) associated with photosynthesis and ecosystem respiration ( $R_{eco}$ ) documented by Boussetta et al. (2013).

These different aspects are discussed in further detail below in Sect. 2.1 to 2.4.

## 2.1 Computation of NEE budget

The biases of the NEE fluxes that we aim to correct are partly linked to model parameter errors that depend on vegetation type and to errors in the meteorological/vegetation state which are region-dependent (e.g. radiation, LAI, temperature and precipitation). In addition to that, the global optimised fluxes used as reference do not currently have a strong constraint from observations at small spatial and temporal scales due to the sparse observing network of atmospheric CO<sub>2</sub>. Therefore, the NEE biases are not diagnosed at the model grid-point scale, but as biases in the NEE budget over continental regions for different vegetation types and over a period of 10 days. The 10-day regional budget provides an indicator on the large-scale biases. Moreover,



10 days is a period that can be used in the current framework of the **CAMS-C-IFS** global atmospheric CO<sub>2</sub> forecasting system. Figure 2 shows how the uncorrected NEE from the past forecasts can be combined to compute the 10-day mean budget before each new forecast. The 1-day forecasts initialised from the previous seven days are used together with the last 3-day forecast available in order to create a 10-day window around the initial date of the new forecast. This 10-day time window is slightly shifted to the past because otherwise forecasts longer than 3-days would be required to compute the budget while errors in the meteorology affecting the fluxes grow with forecast lead time. Chevallier and Kelly (2002) found that forecast errors associated with the location of extra-tropical weather systems affecting the cloud cover and temperature gradients – which in turn will affect the NEE errors – are very small at day 1. These errors continue to be small up to day 3, but they can grow rapidly with forecast lead time (see Haiden et al., 2015, for details on the IFS forecast error evaluation). The different regions have been selected according to latitudinal band characterised by seasonal cycle (northern hemisphere, tropics and southern hemisphere), continental region and vegetation type.

In the IFS the vegetation types follow the BATS classification (Dickinson et al., 1986), which is widely used in meteorological and climate models. The vegetation classification is designed to distinguish between roughness lengths for the computation of the momentum, heat and moisture transfer coefficients in the modelling of the fluxes from surface to atmosphere. However, the BATS vegetation types are not always suitable for the modelling of the CO<sub>2</sub> fluxes. For example, the interrupted forest type which constitutes around 25 % of the high vegetation cover encompasses many different types of vegetation, including Tropical Savanna and a combination of remnants of forest or open woods lands with field complexes. This could be an important source of error in some regions. For this reason, BFAS allows the introduction of new vegetation types for diagnosing the NEE biases. Tropical Savanna which covers large areas in the tropical region has been added as a subtype of the interrupted forest vegetation type by using the Olson Global Ecosystem classification (Olson, 1994a, b, [edc2.usgs.gov/glcc/globdoc2\\_0.php](http://edc2.usgs.gov/glcc/globdoc2_0.php)).

Figure 3 shows the distribution of the dominant vegetation types used in BFAS. Land cover maps from GLCC version 1 ([edc2.usgs.gov/glcc/glcc.php](http://edc2.usgs.gov/glcc/glcc.php)) are used to compute the land cover of the dominant high and low vegetation types at each grid point. In BFAS, only one dominant vegetation type is used to classify each grid point, and this must cover more than 50 % of the grid box. Model grid points with less than 50 % vegetation cover are not used. The comparison of the modelled NEE with the optimised NEE fluxes is done by computing 10-day budgets for each of the 16 vegetation types (see Table 1) and 9 different regions (see Fig. 3).

## 2.2 Reference NEE budget

The residual NEE from optimised fluxes provides the reference for the flux adjustment scheme. Currently, there is no operational centre providing CO<sub>2</sub> optimised fluxes at global scale in near-real time. We have chosen to use the MACC optimised fluxes (Chevallier et al., 2010) which are delivered around September each year for the previous year. The MACC optimised CO<sub>2</sub> fluxes are regularly improved and their high quality has been recently shown by Kulawik et al. (2015). Chevallier (2013) provides an evaluation of the inverted CO<sub>2</sub> fluxes for 2010.

The computation of the residual is done by subtracting the prescribed fluxes used in the **CAMS-C-IFS** CO<sub>2</sub> forecast over land from the total optimised flux. The prescribed CO<sub>2</sub> fluxes from biomass burning and anthropogenic emissions in the CO<sub>2</sub> forecast are not the same as the ones used as prior fluxes in the MACC flux inversion system. Not only they are from different sources, but they are also used at different resolutions. This means that there might be fires represented in one and not the other, or with different emission intensities, as it is the case for anthropogenic hotspots at high versus low resolutions. Thus, in order to avoid the transfer of inconsistencies between the prescribed and prior fluxes into the NEE residual, the regions with very high anthropogenic emissions (larger than  $3 \times 10^6 \text{ g C m}^{-2} \text{ s}^{-1}$ ) and fires are filtered out.

A climatology of these reference NEE fluxes is created using the last 10 available years and it is updated every time a new year is available. Thus, allowing for slow decadal variations in the NEE reference. Figure 4 shows a comparison of the optimised flux budget in 2010 and its climatology for the crop vegetation type in North America. The inter-annual variability of the optimised flux budget is depicted by the standard deviation around the 10-year climatology. The reference NEE climatology is then adjusted to account for the inter-annual variability of the land sink fluxes as follows:

$$f^O = f^{\text{Oclim}} + \gamma \sigma(f^{\text{Oclim}}), \quad (2)$$

where  $f$  is the 10-day NEE budget for a specific region and vegetation type,  $f^O$  is the reference budget,  $f^{\text{Oclim}}$  and  $\sigma(f^{\text{Oclim}})$  are the climatological mean and standard deviation of the optimised flux budget respectively from 2004 to 2013, and  $\gamma$  is the corresponding standardised anomaly of the NEE budget from the model with respect to the same period.  $\gamma$  can be positive or negative. It represents the inter-annual variability factor used to adjust the reference climatological NEE budget and it is given by

$$\gamma = \frac{f^M - f^{\text{Mclim}}}{\sigma(f^{\text{Mclim}})} \quad (3)$$

where  $f^M$  is the model NEE budget,  $f^{\text{Mclim}}$  is the climatological mean budget from the model and  $\sigma(f^{\text{Mclim}})$  is the standard deviation of the model NEE budget denoting the typical amplitude of its inter-annual variability for the same

period as the climatology of the optimised flux budget (i.e. 2004 to 2013).

The  $\gamma$  inter-annual variability factor is multiplied by the standard deviation of the optimised residual NEE budget – representing the typical amplitude of inter-annual variability – in order to offset the reference climatological NEE budget. In this way, the inter-annual variability of the reference NEE follows the inter-annual variability of the model NEE with the same anomaly sign, while keeping its amplitude constrained by the standard deviation of the optimised flux budget. Note that the use of this factor is optional. By setting it to zero, the model budget can be constrained by the optimized flux climatology. The rationale for applying this factor in the C-IFS system is based on the fact that inter-annual variability of the NEE budget is strongly linked to the inter-annual variability of climate variables such as precipitation and temperature (Schaefer et al., 2002). Since information on these climate variables is readily available in the C-IFS system, it is worth exploring its impact on the CO<sub>2</sub> forecast. A preliminary assessment of the impact of including the inter-annual variability factor was performed by comparing experiment with and without the factor. Results confirmed a small but positive impact (see Supplement). Details on the computation of this factor are given in the next section.

### 2.3 The inter-annual variability factor

The computation of the inter-annual variability factor  $\gamma$  requires a model climate consistent with the forecast (i.e. same meteorological analysis, same model version and same resolution). Producing a consistent model climate is not a trivial requirement, because both the operational model version and analysis system can change frequently with new updates and new observations, and high resolution forecasts spanning a period of 10 years (i.e. 2004 to 2013) are expensive. A feasible solution has been found where the standardised NEE anomaly from the model is computed using the operational Ensemble Prediction System (ENS) forecasts and hindcasts which are part of the ECMWF monthly forecasting system (Vitart et al., 2008; Vitart, 2013, 2014). Every Monday and Thursday the operational ENS is not only run for the actual date, but also for the same calendar day of the past 20 years. These hindcasts have the same resolution and model version as the ENS forecasts and they constitute a valuable data set used for the post-processing and calibration of the NWP forecasts from the medium-range (10 days) up to one month lead times (Hagedorn et al., 2012). The ensemble of forecasts is made of 5 members (10 members since 2015) using perturbed initial conditions (Lang et al., 2015) and stochastic physics in order to represent forecast uncertainty (Palmer et al., 2009).

As the hindcasts are not performed daily, it is not possible to aggregate consecutive 1-day forecasts into a 10-day period to compute a mean budget as shown in Fig. 2. In order to circumvent this, the mean budget is computed by averaging the

1-day forecast NEE from all the ensemble members available in the hindcasts. This is done for each year from 2004 to 2013 to preserve consistency with the NEE climatology from the optimised fluxes. The model climate  $f^{\text{Mclim}}$  given by the 10-year mean budget and its typical inter-annual variability  $\sigma(f^{\text{Mclim}})$  can then be obtained by calculating the mean value and standard deviation respectively over that period. Similarly, the model budget  $f^{\text{M}}$  is calculated from the NEE ensemble mean of the ENS forecast for the current date using the same number of ensemble members as the ENS hindcasts. The standardised anomaly  $\gamma$  is finally obtained by subtracting the 10-year mean budget from the current budget and dividing the anomaly by the standard deviation. Since the hindcasts are available every Monday and Thursday,  $\gamma$  is only updated twice a week. These updates are routinely monitored during the forecast (see Sect. 4).

### 2.4 Partition of NEE adjustment

The final stage in the flux adjustment is the attribution of the NEE correction to the different biogenic fluxes in the model. The residual NEE from optimised fluxes only provides information on the total flux from the land ecosystem exchange. While in land vegetation models, NEE is the combination of two opposing fluxes: Gross Primary Production (GPP) and the ecosystem respiration ( $R_{\text{eco}}$ ). Given that we have no information on whether the NEE error is associated with the GPP or the  $R_{\text{eco}}$  fluxes, a strategy has to be defined in order to partition the NEE correction into GPP and  $R_{\text{eco}}$ . The underlying strategy used here is to have the smallest flux adjustment possible. Namely, the scaling factors should be as close to 1 as possible.

The first step is to distinguish between the positive and negative values of the NEE scaling factor ( $\alpha$ ). A positive NEE scaling factor implies the budget of the NEE in the model has the correct sign but the wrong magnitude. In that case, the scaling of the flux will be smallest if the dominant component of NEE is scaled. That is to say, the flux correction will be applied to GPP during the growing season and to  $R_{\text{eco}}$  during the senescence period. Whereas if the scaling factor is negative – i.e. the modelled NEE has the wrong sign – only the flux with smallest magnitude is corrected (GPP or  $R_{\text{eco}}$ ) to ensure the scaling factor of the modelled fluxes is always positive.

The scaling factor  $\alpha$  is then converted into a scaling factor for the dominant component of the NEE flux. If the magnitude of GPP is larger than the magnitude of  $R_{\text{eco}}$ , then the scaling factor for GPP and  $R_{\text{eco}}$  are defined as follows:

$$\begin{aligned}\alpha_{\text{GPP}} &= \frac{\alpha \text{NEE} - R_{\text{eco}}}{\text{GPP}} \\ \alpha_{R_{\text{eco}}} &= 1.0\end{aligned}\quad (4)$$

Similarly, if  $|R_{\text{eco}}| > |\text{GPP}|$  then

$$\alpha_{\text{GPP}} = 1.0$$

$$\alpha_{R_{\text{eco}}} = \frac{\alpha_{\text{NEE}} - \text{GPP}}{R_{\text{eco}}} \quad (5)$$

This partition the flux adjustment is a modelling choice based on minimum flux adjustment criteria. Other solutions might be possible given additional information on either GPP or  $R_{\text{eco}}$  budgets.

The  $\alpha_{\text{GPP}}$  and  $\alpha_{R_{\text{eco}}}$  factors are computed for each vegetation type and region and then re-mapped as 2-d fields using the dominant vegetation type map in Fig. 3. The resulting maps for  $\alpha_{\text{GPP}}$  and  $\alpha_{R_{\text{eco}}}$  are subsequently passed to the carbon module in the land surface model in order to scale GPP and  $R_{\text{eco}}$ .

### 3 CO<sub>2</sub> forecast simulations

Several simulations have been performed in order to test the impact of BFAS on the atmospheric CO<sub>2</sub> forecasts (see Table 2). All the simulations use the CAMS C-IFS CO<sub>2</sub> forecasting system (Agustí-Panareda et al., 2014) based on the IFS model ([www.ecmwf.int/en/forecasts/documentation-and-support](http://www.ecmwf.int/en/forecasts/documentation-and-support)). They all share the same transport. The only difference between them is the CO<sub>2</sub> surface fluxes they use as described in Table 2. The impact of BFAS is assessed by comparing the simulations using modelled NEE fluxes without BFAS (CTRL) and with BFAS (BFAS). The BFAS simulation is also compared with the simulations using optimised fluxes (OPT) and a climatology of optimised fluxes (OPT-CLIM). Both OPT and OPT-CLIM simulations constitute a benchmark because they are driven by the reference fluxes used in BFAS. From these experiments we expect to see the forecast from BFAS to be closer to the benchmark forecasts (in particular CLIM-OPT/OPT-CLIM) than to the CTRL forecast.

The forecasts are performed using the cyclic configuration described by Agustí-Panareda et al. (2014) with a spectral resolution of TL255, equivalent to around 80 km in the horizontal, and 60 vertical levels. They are initialised daily at 00:00 UTC with ECMWF operational analysis, while the atmospheric CO<sub>2</sub> is cycled from one forecast to the next, as in a free run. The simulations span the period from 1 January to 31 December 2010. This period has been selected because of the large variety of observations available to evaluate the BFAS performance on the atmospheric CO<sub>2</sub> forecasts. The CO<sub>2</sub> initial conditions on 1 January 2010 are from the atmospheric CO<sub>2</sub> analysis using GOSAT CO<sub>2</sub> retrievals (Heymann et al., 2015).

### 4 Monitoring the flux adjustment

The flux adjustment is monitored by plotting time series of the flux scaling factors for each vegetation type and region.

For example, Fig. 5 shows the GPP and  $R_{\text{eco}}$  scaling factors for the crop vegetation type which is present in all regions. The values range from 0.5 to 6. These coefficients are computed daily before the beginning of each forecast and they are kept constant throughout the forecast. Generally, there is a slow variation of the coefficients from one day to the next. This is expected since the coefficients are obtained from large-scale budgets computed over a 10-day period. The map of the GPP and  $R_{\text{eco}}$  scaling factors applied to adjust the modelled biogenic fluxes on 15 March 2010 is shown in Fig. 6. These maps can be very useful to monitor the flux adjustment because they can provide alerts on the regions with largest biases to model developers.

The effect of the flux adjustment on the NEE budget is shown in Fig. 7. The adjusted biogenic fluxes should always lead to an NEE budget close to the budget of the optimised NEE climatology. However, the fit will also depend on the degree of inter-annual variability of the model determined by parameter  $\gamma$  in Eq. (3). Figure 8 displays the monitoring of  $\gamma$  given by the standardised NEE anomaly of the model. Positive values mean the CO<sub>2</sub> source is larger than normal and/or the CO<sub>2</sub> sink is lower than normal with respect to the 10-year mean budget of the model, covering the same period as the reference climatology. Conversely, negative values correspond to a smaller than normal source and/or larger than normal sink. When  $\gamma$  is larger than 1, the model anomaly is larger than  $1\sigma$ . This indicates the possible occurrence of an extreme event. Prolonged extreme events – such as droughts – would have an effect on the NEE budget and the computation of the biogenic flux adjustment.

### 5 Impact of the flux adjustment

The impact of BFAS is shown by comparing the atmospheric CO<sub>2</sub> from the BFAS forecast to the CTRL forecast, and to the benchmark forecasts with optimised fluxes (OPT and CLIM-OPT/OPT-CLIM) at several observing sites. Four sites from the NOAA/ESRL atmospheric baseline observatories ([www.esrl.noaa.gov/gmd/obop](http://www.esrl.noaa.gov/gmd/obop), Thoning et al., 2012) are used to evaluate the reduction of the large-scale biases in the well-mixed background air. In addition, four Total Carbon Column Observing Network stations (GGG2014 TC-CON data, Wunch et al., 2011, see Table 3 and [www.tccon.caltech.edu](http://www.tccon.caltech.edu)) are also used to assess the impact on the atmospheric CO<sub>2</sub> column-average dry molar fraction. Finally, three continental sites from the NOAA/ESRL tall tower network ([www.esrl.noaa.gov/gmd/ccgg/towers](http://www.esrl.noaa.gov/gmd/ccgg/towers), Andrews et al., 2014) are used to investigate the impact of BFAS on the synoptic skill of the forecasts. The results are grouped into the impacts on bias reduction and synoptic skill in the following two sections. [A comprehensive evaluation of the uncertainty reduction in the BFAS simulation based on all the ObsPack \(2015\) in situ flask and continuous observations,](#)

as well as the NOAA/ESRL aircraft vertical profiles (Sweeney et al., 2015) is also provided in the Supplement.

## 5.1 Biases in atmospheric CO<sub>2</sub>

Figure 9 demonstrates that BFAS is very effective at reducing the atmospheric CO<sub>2</sub> biases in the background air at all the NOAA/ESRL continuous baseline stations. The biases in the CTRL forecast range from  $-1.9$  to  $-4.5$  ppm; whereas, the BFAS forecast has biases of  $-0.5$  ppm or less over the whole year. These values are close to the annual biases of the OPT and OPT-CLIM experiments ranging between  $-0.4$  and  $0.5$  ppm. The monthly biases in BFAS can be larger than its annual biases. For example, there is a bias of up to  $-1$  ppm from March to September in the southern hemisphere (Fig. 9c, d). This bias is thought to originate in the tropical regions and transported to the southern hemisphere as shown by a preliminary comparison with IASI CO<sub>2</sub> (Crevoisier et al., 2009) (not shown here). The bias starts to grow at the end of the growing season during summer time. This is also the case for the high latitude station at Barrow, where there is a negative bias of a few ppm from the last week of July to the end of September as shown in Fig. 9a. In summary, BFAS is not able to completely remove the negative model bias at the end of the growing season. In the northern hemisphere at the end of winter and throughout spring (from March to May) there is a positive model bias, i.e. the atmospheric CO<sub>2</sub> is overestimated in the model. Although the OPT and OPT-CLIM simulations also have a slight positive bias in winter, this positive bias is enhanced in the BFAS simulation.

At the TCCON sites (Fig. 10), the atmospheric CO<sub>2</sub> column-average dry molar fraction also shows the same large bias reduction in BFAS with respect to CTRL. The magnitude of the BFAS annual biases in the atmospheric column is generally less than 1 ppm, slightly higher than the OPT and OPT-CLIM biases (less than 0.5 ppm), but much lower than the CTRL biases (from 1.5 to 3.3 ppm). The results at the TCCON sites are consistent with those from the NOAA/ESRL baseline sites. Namely, in the northern hemisphere there is a growing overestimation of the atmospheric CO<sub>2</sub> at the end of winter (around March). While at the end of the growing season in both northern and southern hemispheres (August and March respectively) there is a growing negative bias, i.e. an overestimation of the sink. One hypothesis that could explain why BFAS is not able to achieve as small a bias as the forecast with optimised fluxes lies in the fact that the optimised NEE used as a reference in BFAS is computed as a residual after removing the effect of fires and anthropogenic fluxes. Inconsistencies in the fire and anthropogenic emissions used by the optimised fluxes and the model will lead to errors in the optimised residual NEE. These inconsistencies are mainly associated with the use of different resolutions. Further investigation is required to address this issue.

## 5.2 Synoptic variability of atmospheric CO<sub>2</sub>

The CO<sub>2</sub> forecast has been shown to have high skill in simulating the synoptic variability of atmospheric CO<sub>2</sub> (see Agustí-Panareda et al., 2014), except during the spring months, coinciding with an early start of the CO<sub>2</sub> drawdown period in the model. For this reason, we have examined the impact of BFAS on the synoptic variability of daily mean atmospheric CO<sub>2</sub> at three continental NOAA/ESRL tower sites in March. Over this period, the day-to-day variability of atmospheric CO<sub>2</sub> at those sites is associated with the advection of atmospheric CO<sub>2</sub> by baroclinic synoptic weather systems as they impinge on the large-scale continental gradient of atmospheric CO<sub>2</sub>. Table 4 clearly demonstrates that with BFAS the synoptic forecast skill is greatly improved at all sites, with correlation coefficients between simulated and observed atmospheric CO<sub>2</sub> exceeding 0.8. The improvement is particularly striking at Park Falls (Wisconsin, USA) and West Branch (Iowa, USA) at the centre of North America, where the correlation coefficients in CTRL are very low (i.e. below 0.5). The OPT and OPT-CLIM forecasts have generally high correlation coefficients, comparable to BFAS. Only at the level closest to the surface, the values are slightly lower than BFAS. This can be explained by the fact that the MACC-13R1 optimised fluxes do not comprise synoptic variability. Thus, when the synoptic variability of the fluxes contributes to the atmospheric CO<sub>2</sub> variability, the correlation coefficients are smaller.

The positive impact of BFAS on the CO<sub>2</sub> synoptic variability is illustrated in Fig. 11. The large synoptic variability is characterised by the advection of CO<sub>2</sub>-rich anomalies (with up to 10 ppm amplitude) as shown by the CO<sub>2</sub> peaks on 10–12 March at Park Falls, and 8–9, 12–13 and 16–17 March at West Branch. These CO<sub>2</sub> anomalies originate from the advection across the large-scale continental gradients of atmospheric CO<sub>2</sub> which ultimately reflect the large-scale distribution of CO<sub>2</sub> surface fluxes (Keppel-Aleks et al., 2012). In the case study here, the CO<sub>2</sub>-rich air is located to the south of the observing stations, as shown by the distribution of the monthly mean atmospheric CO<sub>2</sub> depicting the large-scale gradients across the continent at the level corresponding to the height of the tall towers (Figs. 12a and 12b). In the CTRL forecast, there is no monthly mean gradient south of the stations (Fig. 12c). This explains why without BFAS the synoptic variability is very small and largely underestimated throughout March. While in BFAS the gradient south of the observing stations is very pronounced (Fig. 12d), following a similar pattern to OPT and OPT-CLIM. There are still some differences between the three simulations. OPT-CLIM results in stronger gradients than OPT and BFAS enhances the gradient even further, leading to a slight overestimation of the synoptic variability. These differences in the patterns of the atmospheric CO<sub>2</sub> are directly linked to the differences in the CO<sub>2</sub> surface fluxes (Fig. 13). As expected, the flux adjustment from BFAS results in a flux pattern sim-



ilar to OPT-CLIM and OPT, with a stronger source to the south of the observing stations. Whereas in CTRL there is a large sink area south of the observing stations, in the region of the Gulf of Mexico, consistent with the CTESSEL early growing season (Balzarolo et al., 2014).

## 6 Discussion

All the results from the BFAS experiments indicate that BFAS is highly beneficial to the ~~CAMS-C-IFS~~ CO<sub>2</sub> forecasting system, both in terms of reducing the atmospheric CO<sub>2</sub> biases and improving the synoptic skill of the model. As shown in Sect. 2, the scheme is simple and it is easy to implement and run. Because BFAS essentially works as a layer on top of the model, it can adapt to model changes with great flexibility. For all these reasons, BFAS is now part of the operational global ~~CAMS-C-IFS~~ analysis and forecasting system.

Notwithstanding all the advantages of BFAS listed above, there are also caveats that need to be considered, further tested and addressed. A discussion of the current limitations of BFAS is provided in this section, together with the potential use of BFAS for model development and data assimilation purposes and the implications for users.

### 6.1 Current limitations in BFAS

Optimised fluxes have uncertainties of their own and represent the large-scale variability of the CO<sub>2</sub> surface fluxes on supra-synoptic time-scales. They only estimate the total flux and the NEE residual approach can transfer biases from other fluxes into the NEE. The use of a climatology also precludes the correction of the inter-annual variability in the model.

The aggregation criteria of budget errors can be very challenging because the error can originate from different aspects of the model. Clearly, errors in model parameters associated with vegetation type are a good candidate. However, in the future errors in climate forcing, errors in LAI, missing processes and other potential sources of error should also be considered.

The partition of the NEE flux adjustment into the modelled biogenic fluxes (GPP and  $R_{eco}$ ) is currently ad-hoc, leading to the transfer of errors from GPP to  $R_{eco}$  and vice-versa. This problem could be addressed by using other independent datasets of GPP and  $R_{eco}$  (e.g. Jung et al., 2011) that contain additional information on how to partition the NEE adjustment.

### 6.2 BFAS for model development

BFAS can run in both online and offline modes. Thus, it can provide a tool to diagnose regions that contribute to the errors in the global budget resulting in large-scale errors of atmospheric CO<sub>2</sub>. The maps of biogenic flux scaling factors can be used to compute maps of flux adjustment (e.g. ad-

justed NEE – original NEE) which can then be used to diagnose model errors. The synthesis of the mean adjustments into monthly model biases for different vegetation types can then guide the effort to develop the carbon model further. For example, in regions where the bias is consistent between different months, the corrected NEE could be used to re-tune model parameters such as the reference ecosystem respiration or the mesophyll conductance, previously optimised by Boussetta et al. (2013) using a subset of FLUXNET data. Specific vegetation types can be identified where model improvements could be achieved by using information from BFAS. For instance, crops have the same large  $R_{eco}$  scaling ( $> 1.5$ ) over all the northern hemisphere regions during winter months when the ecosystem respiration is the dominant component of NEE. This underestimation in the ecosystem respiration can be addressed by modifying the value of the reference respiration parameter used for crops. In this case, the same procedure used by Boussetta et al. (2013) could be applied to optimise the specific model parameter using the BFAS adjusted fluxes as pseudo-observations together with the FLUXNET data.

Further information on error sources in fluxes can be obtained by comparing the corrected fluxes with the eddy covariance observations available in near-real time from the Integrated Observation System (ICOS) Ecosystem Thematic Centre (ETC, <http://www.europe-fluxdata.eu>). For example, preliminary comparisons have shown that there are large differences in the model-observation fit between needle leaf evergreen (pine) trees in the boreal and Mediterranean regions. This is consistent with results from Balzarolo et al. (2014), and it highlights the need for a new sub-classification of the evergreen needle leaf forests in regions with Mediterranean climate.

### 6.3 BFAS in the data assimilation framework

Currently, BFAS is only designed to be used as a bias correction computed before each forecast by using a reference data set based on optimised fluxes. In the future, BFAS could be adapted to work within a data assimilation (DA) framework in the IFS. To start with, the ~~use-specification~~ of uncertainties associated with both the reference data set and the model fluxes and the covariance of those uncertainties would allow a more optimal estimation of the flux adjustment. These uncertainties can be obtained from the flux inversion systems for the optimised fluxes and from the ECMWF ENS forecasts for the model fluxes.

Including BFAS in the IFS DA framework needs further exploration. The IFS uses a short time window (currently 12 h) to assimilate meteorological observations from very dense observing networks. With the short time window it is not possible to properly constrain the slowly varying global mass of the long-lived greenhouse gases due to the sparseness of their observing system. For instance, the current GOSAT and OCO-2 CO<sub>2</sub> observations do not cover high

latitudes in winter. However, if we combined the assimilation of optimised fluxes (which already contain the global mass constraint) with observations linked to local fluxes (e.g. solar-induced chlorophyll fluorescence products from satellites, NEE eddy covariance observations and in situ atmospheric CO<sub>2</sub> observations) it might be possible to obtain an optimal estimate of more local scaling factors, while still respecting the global mass constraint. The possibility of optimising the scaling factors in the DA system within the weak constraint framework (Trémolet, 2006, 2007) also needs to be explored in the future.

#### 6.4 Aspects to be considered by users

The implementation of BFAS is straightforward. Therefore, it could be easily used by other models. The only requirements are: (i) a reference budget which can be obtained from a climatology of optimized fluxes (e.g. the MACC product can be easily obtained from [www-lscedods.cea.fr/invsat/PYVAR14\\_MACC/V2/Fluxes/3Hourly](http://www-lscedods.cea.fr/invsat/PYVAR14_MACC/V2/Fluxes/3Hourly) and it is well documented); (ii) past 10-day NEE simulated by the forward model; (iii) the NEE anomaly of the forward model with respect to its climate based on a 10-year simulation. The use of the NEE anomaly is optional, as its impact is relatively small (see Supplement).

The underlying motivation of BFAS is to improve the CO<sub>2</sub> analysis and forecast for users (e.g. those working on flux inversion systems, planning field experiments, or requiring boundary conditions for regional models). For this reason, it is paramount to provide information on all the input data going into BFAS. These are primarily continental-scale climatological budgets from modelled NEE and optimized fluxes. There is also some input from the anthropogenic emissions and the biomass burning emissions to extract the NEE as a residual from the optimized fluxes. The documentation of the specific components used in the C-IFS BFAS system and their uncertainties can be found in Boussetta et al. (2013), Chevallier et al. (2010); Chevallier (2015), Janssens-Maenhout et al. (2012) and Kaiser et al. (2012). The input data streams used in BFAS can be obtained from <http://copernicus-support.ecmwf.int> for C-IFS NEE and GFAS biomass burning fluxes; from the EDGAR database <http://edgar.jrc.ec.europa.eu> for the anthropogenic fluxes; and from [www-lscedods.cea.fr/invsat/PYVAR14\\_MACC/V2/Fluxes/3Hourly](http://www-lscedods.cea.fr/invsat/PYVAR14_MACC/V2/Fluxes/3Hourly) for the MACC optimized fluxes.

Since the BFAS product contains information from the optimized fluxes, users should be aware that the optimized fluxes assimilated most available background air-sample monitoring sites (listed in the supplement of Chevallier (2015), see <http://www.atmos-chem-phys.net/15/11133/2015/acp-15-11133-2015-supplement.pdf>). A specification of the overall uncertainty associated with the BFAS simulation and the resulting reduction with respect to the control simulation is given in the Supplement.

## 7 Summary

~~A new biogenic flux adjustment scheme (BFAS) has been developed at ECMWF to reduce large-scale biases of the ecosystem fluxes modelled by the CTESSEL carbon model.~~ This paper addresses the challenge of designing an online bias correction for an atmospheric CO<sub>2</sub> analysis/forecasting system. The overarching aim is to deliver an atmospheric CO<sub>2</sub> analysis and forecast that can be useful to the scientific community, e.g. working on data assimilation of atmospheric CO<sub>2</sub> observations, the development of the CO<sub>2</sub> observing system and providing boundary conditions for CO<sub>2</sub> regional modelling. Tuning model parameters and/or re-scaling fluxes offline are not sufficient to guarantee a bias reduction in the system. Thus, an online adaptive system is required because errors in the meteorology can evolve as a result of regular operational NWP model upgrades and these affect the NEE budget in the model. This is achieved in the new biogenic flux adjustment scheme (BFAS) by a simple scaling of the 10-day NEE budgets for different vegetation types and regions using a climatology of the MACC optimised fluxes (Chevallier et al., 2010) as a reference, adjusted to preserve the model inter-annual variability.

This paper shows that BFAS has a positive impact on the atmospheric CO<sub>2</sub> forecast by greatly reducing the atmospheric CO<sub>2</sub> biases in background air and improving the synoptic variability in continental regions affected by ecosystem fluxes. The improvement in the synoptic skill of the forecast is associated with underlying changes in the large-scale gradient of the NEE fluxes where optimised fluxes provide information. ~~Because~~

~~BFAS has been recently implemented in the C-IFS operational CO<sub>2</sub> forecast and analysis system, because of its simplicity, adaptability to model changes and beneficial impact, BFAS has been recently implemented in the CAMS operational CO<sub>2</sub> forecast and analysis system.~~ In this paper, the C-IFS model is just providing an example on how this method can be applied efficiently in an operational forecasting system. Other models could easily adopt such a system as there are only a few components required for its implementation (see section 6.4).

As a diagnostic tool, BFAS has also ~~potential~~ the potential to provide feedback for model development. The use of BFAS in the data assimilation framework will be explored in the future.

**Acknowledgements.** This study has been funded by the European Commission under the Monitoring of Atmospheric Composition and Climate (MACC) project and the Copernicus Atmosphere Monitoring Service (CAMS).

TCCON data were obtained from the TCCON Data Archive, hosted by the Carbon Dioxide Information Analysis Center (CDIAC) – [tcon.onrll.gov](http://tcon.onrll.gov). The authors would like to acknowledge the PIs of the different TCCON stations used in this study: Rigel Kivi (Sodankylä, Finland), Nicholas Deutscher (Bialystok,

Poland), Paul Wennberg (Lamont, USA) and David Griffith (Wollongong, Australia).

We acknowledge Ed Dlugokencky and Arlene Andrews (NOAA/ESRL) for the NOAA/ESRL data. The NOAA/ESRL Global Monitoring Division data from the baseline observatories at Barrow (Alaska, USA), Mauna Loa (Hawaii, USA), American Samoa (USA), South Pole (Antarctica), as well as the tall towers at Argyle (Maine, USA), Park Falls (Wisconsin, USA) and West Branch (Iowa, USA) were obtained from [ftp://ftp.cmdl.noaa.gov/data/greenhouse\\_gases/co2](ftp://ftp.cmdl.noaa.gov/data/greenhouse_gases/co2). We acknowledge Colm Sweeney (NOAA/ESRL) for the NOAA/ESRL aircraft profiles and all the laboratories contributing to the compilation of ObsPack (2015).

The authors are very grateful to Nils Wedi for his support in processing the Olson ecosystem classification maps and to Fredéric Vitard for providing support and advice on the use of the ENS hindcasts. We would also like to acknowledge the comments from Peter Rayner and an anonymous reviewer which helped improve the message and documentation of the atmospheric CO<sub>2</sub> error reduction associated with the flux adjustment presented in the paper.

## References

- Agustí-Panareda, A., Massart, S., Chevallier, F., Boussetta, S., Balsamo, G., Beljaars, A., Ciais, P., Deutscher, N. M., Engelen, R., Jones, L., Kivi, R., Paris, J.-D., Peuch, V.-H., Sherlock, V., Vermeulen, A. T., Wennberg, P. O., and Wunch, D.: Forecasting global atmospheric CO<sub>2</sub>, *Atmos. Chem. Phys.*, 14, 11959–11983, doi:10.5194/acp-14-11959-2014, 2014.
- Andrews, A. E., Kofler, J. D., Trudeau, M. E., Williams, J. C., Neff, D. H., Masarie, K. A., Chao, D. Y., Kitzis, D. R., Novelli, P. C., Zhao, C. L., Dlugokencky, E. J., Lang, P. M., Crotwell, M. J., Fischer, M. L., Parker, M. J., Lee, J. T., Baumann, D. D., Desai, A. R., Stanier, C. O., De Wekker, S. F. J., Wolfe, D. E., Munger, J. W., and Tans, P. P.: CO<sub>2</sub>, CO, and CH<sub>4</sub> measurements from tall towers in the NOAA Earth System Research Laboratory's Global Greenhouse Gas Reference Network: instrumentation, uncertainty analysis, and recommendations for future high-accuracy greenhouse gas monitoring efforts, *Atmos. Meas. Tech.*, 7, 647–687, doi:10.5194/amt-7-647-2014, 2014.
- Balzarolo, M., Boussetta, S., Balsamo, G., Beljaars, A., Maignan, F., Calvet, J.-C., Lafont, S., Barbu, A., Poulter, B., Chevallier, F., Szczypta, C., and Papale, D.: Evaluating the potential of large-scale simulations to predict carbon fluxes of terrestrial ecosystems over a European Eddy Covariance network, *Biogeosciences*, 11, 2661–2678, doi:10.5194/bg-11-2661-2014, 2014.
- Boussetta, S., Balsamo, G., Beljaars, A., Agustí-Panareda, A., Calvet, J.-C., Jacobs, C., van den Hurk, B., Viterbo, P., Lafont, S., Dutra, E., Jarlan, L., Balzarolo, M., Papale, D., and van der Werf, G.: Natural carbon dioxide exchanges in the ECMWF Integrated Forecasting System: Implementation and offline validation, *J. Geophys. Res.-Atmos.*, 118, 1–24, doi:10.1002/jgrd.50488, 2013.
- Chen, Z. H., Zhu, J. and Zeng, N.: Improved simulation of regional CO<sub>2</sub> surface concentrations using GEOS-Chem and fluxes from VEGAS, *Atmospheric Chemistry and Physics*, 13, 7607–7618, doi:10.5194/acp-13-7607-2013, 2013.
- Chevallier, F., On the statistical optimality of CO<sub>2</sub> atmospheric inversions assimilating CO<sub>2</sub> column retrievals, *Atmospheric Chemistry and Physics*, 15, 11133–11145, doi:10.5194/acp-15-11133-2015, 2015.
- Chevallier, F.: Report on the quality of the inverted CO<sub>2</sub> fluxes, MACC-II deliverable D\_043.4, ECMWF, available at: [http://www.gmes-atmosphere.eu/documents/maccii/deliverables/ghg/MACCII\\_GHG\\_DEL\\_D43.4\\_20120430\\_Chevallier.pdf](http://www.gmes-atmosphere.eu/documents/maccii/deliverables/ghg/MACCII_GHG_DEL_D43.4_20120430_Chevallier.pdf) (last access: 21 December 2015), 2013.
- Chevallier, F. and Kelly, G.: Model clouds as seen from space: comparison with geostationary imagery in the 11-m window channel, *Mon. Weather Rev.*, 130, 712–722, 2002.
- Chevallier, F., Ciais, P., Conway, T., Aalto, T., Anderson, B., Bousquet, P., Brunke, E., Ciattaglia, L., Esaki, Y., Fröhlich, M., Gomez, A., Gomez Pelaez, A., Haszpra, L., Krummel, P., Langenfelds, R., Leuenberger, M., Machida, T., Maignan, F., Matsueda, H., Morgu, J., Mukai, H., Nakazawa, T., Peylin, P., Ramonet, M., Rivier, L., Sawa, Y., Schmidt, M., Steele, L., Vay, S., Vermeulen, A., Wofsy, S., and Worthy, D.: CO<sub>2</sub> surface fluxes at grid point scale estimated from a global 21 year reanalysis of atmospheric measurements, *J. Geophys. Res.*, 115, D21307, doi:10.1029/2010JD013887, 2010.
- Crevoisier C., Chédin A., Scott N. A., Matsueda H., Machida T., and Armante R.: First year of upper tropospheric integrated content of CO<sub>2</sub> from IASI hyperspectral infrared observations, *Atmos. Chem. Phys.*, 9, 4797–4810, 2009.
- Ciais, P., Dolman, A. J., Bombelli, A., Duren, R., Peregon, A., Rayner, P. J., Miller, C., Gobron, N., Kinderman, G., Marland, G., Gruber, N., Chevallier, F., Andres, R. J., Balsamo, G., Bopp, L., Bréon, F.-M., Broquet, G., Dargaville, R., Battin, T. J., Borges, A., Bovensmann, H., Buchwitz, M., Butler, J., Canadell, J. G., Cook, R. B., DeFries, R., Engelen, R., Gurney, K. R., Heinze, C., Heimann, M., Held, A., Henry, M., Law, B., Luysaert, S., Miller, J., Moriyama, T., Moulin, C., Myneni, R. B., Nussli, C., Obersteiner, M., Ojima, D., Pan, Y., Paris, J.-D., Piao, S. L., Poulter, B., Plummer, S., Quegan, S., Raymond, P., Reichstein, M., Rivier, L., Sabine, C., Schimel, D., Tarasova, O., Valentini, R., Wang, R., van der Werf, G., Wickland, D., Williams, M., and Zehner, C.: Current systematic carbon-cycle observations and the need for implementing a policy-relevant carbon observing system, *Biogeosciences*, 11, 3547–3602, doi:10.5194/bg-11-3547-2014, 2014.
- Denning, S., Oren, R., McGuire, D., Sabine, C., Doney, S., Paustian, K., Torn, M., Dilling, L., Heath, L., Tans, P., Wofsy, S., Cook, R., Waltman, S., Andrews, A., Asner, G., Baker, J., Bakwin, P., Birdsey, R., Crisp, D., Davis, K., Field, C., Gerbig, C., Hollinger, D., Jacob, D., Law, B., Lin, J., Margolis, H., Marland, G., Mayeux, H., McClain, C., McKee, B., Miller, C., Pawson, S., Randerson, J., Reilly, J., Running, S., Saleska, S., Stallard, R., Sundquist, E., Ustin, S., and Verma, S.: Science implementation strategy for the North American Carbon Program, Report on the NACP Implementation Strategy Group of the U.S. Carbon Cycle Interagency Working Group, Washington, DC, USA, U.S. Carbon Cycle Science Program, 2005.
- Deutscher, N., Notholt, J., Messerschmidt, J., Weinzierl, C., Warneke, T., Petri, C., Grupe, P., and Katrynsk, K.: TC-CON data from Bialystok, Poland, Release GGG2014R0., Tech. rep., TCCON data archive, hosted by the Carbon Dioxide Information Analysis Center, Oak Ridge National Laboratory, Oak Ridge, Tennessee, USA., doi:10.14291/tcon.ggg2014.bialystok01.R0/1149277, 2014.



- Dickinson, R., Henderson-Sellers, A., Kennedy, P., and Wilson, M.: Biosphere-atmosphere transfer scheme (BATS) for the NCAR community model, Ncar technical note, NCAR, nCAR/TN-275+STR NOAA, doi:10.5065/D6668B58, 1986.
- Flemming, J., Inness, A., Flentje, H., Huijnen, V., Moinat, P., Schultz, M. G., and Stein, O.: Coupling global chemistry transport models to ECMWF's integrated forecast system, *Geosci. Model Dev.*, 2, 253–265, doi:10.5194/gmd-2-253-2009, 2009.
- Griffith, D. W. T., Velazco, V. A., Deutscher, N., Murphy, C., Jones, N., Wilson, S., Macatangay, R., Kettlewell, G., Buchholz, R. R., and Riggensbach, M.: TCCON data from Wollongong, Australia, Release GGG2014R0, Tech. rep., TCCON data archive, hosted by the Carbon Dioxide Information Analysis Center, Oak Ridge National Laboratory, Oak Ridge, Tennessee, USA, doi:10.14291/tcon.ggg2014.wollongong01.R0/1149291, 2014.
- Gurney, K., Law, R., Denning, A., Rayner, P., Baker, D., Bousquet, P., Bruhwiler, L., Chen, Y.-H., Ciais, P., Fan, S., Fung, I., Gloor, M., Heimann, M., Higuchi, K., John, J., Maki, T., Maksyutov, S., Masarie, K., Peylin, P., Prather, M., Pak, B., Sarmiento, J., Taguchi, S., Takahashi, T., and Yuen, C.-W.: TransCom3 CO<sub>2</sub> inversion intercomparison: 1. Annual mean control results and sensitivity to transport and prior flux information, *Tellus B*, 55, 555–579, 2003.
- Hagedorn, R., Buizza, R., Hamill, M., Leutbecher, M., and Palmer, T.: Comparing TIGGE multi-model forecasts with re-forecast calibrated ECMWF ensemble forecasts, *Q. J. R. Meteor. Soc.*, 138, 1814–1827, 2012.
- Haiden, T., Janousek, M., Bauer, P., Bidlot, J., Dahoui, M., Ferranti, L., Prates, F., Richardson, D., and Vitar, F.: Evaluation of ECMWF forecasts, including 2014–2015 upgrades, Technical Report 765, ECMWF, available at: [www.ecmwf.int/en/elibrary/miscellaneous/14691-evaluation-ecmwf-forecasts-including-2014-2015-upgrades](http://www.ecmwf.int/en/elibrary/miscellaneous/14691-evaluation-ecmwf-forecasts-including-2014-2015-upgrades) (last access: 5 January 2016), 2015.
- Heymann, J., Reuter, M., Hilker, M., Buchwitz, M., Schneising, O., Bovensmann, H., Burrows, J. P., Kuze, A., Suto, H., Deutscher, N. M., Dubey, M. K., Griffith, D. W. T., Hase, F., Kawakami, S., Kivi, R., Morino, I., Petri, C., Roehl, C., Schneider, M., Sherlock, V., Sussmann, R., Velazco, V. A., Warneke, T., and Wunch, D.: Consistent satellite XCO<sub>2</sub> retrievals from SCIAMACHY and GOSAT using the BESD algorithm, *Atmos. Meas. Tech.*, 8, 2961–2980, doi:10.5194/amt-8-2961-2015, 2015.
- Houweling, S., Baker, D., Basu, S., Boesch, H., Butz, A., Chevallier, F., Deng, F., Dlugokencky, E. J., Feng, L., Ganshin, A., Hasekamp, O., Jones, D., Maksyutov, S., Marshall, J., Oda, T., O'Dell, C. W., Oshchepkov, S., Palmer, P. I., Peylin, P., Poussi, Z., Reum, F., Takagi, H., Yoshida, Y., and Zhuravlev, R.: An intercomparison of inverse models for estimating sources and sinks of CO<sub>2</sub> using GOSAT measurements, *J. Geophys. Res.-Atmos.*, 120, 5253–5266, doi:10.1002/2014JD022962, 2015.
- Janssens-Maenhout, G., Dentener, F., Aardenne, J. V., Monni, S., Pagliari, V., Orlandini, L., Klimont, Z., Kurokawa, J., Akimoto, H., Ohara, T., Wankmueller, R., Battye, B., Grano, D., Zuber, A., and Keating, T.: EDGAR-HTAP: a Harmonized Gridded Air Pollution Emission Dataset Based on National Inventories, JRC68434, EUR report No EUR 25 299-2012, ISBN 978-92-79-23122-0, ISSN 1831-9424, European Commission Publications Office, Ispra, Italy, 2012.
- Jung, M., Reichstein, M., Margolis, H. A., Cescatti, A., Richardson, A. D., Arain, M. A., Arneth, A., Bernhofer, C., Bonal, D., Chen, J., Gianelle, D., Gobron, N., Kiely, G., Kutsch, W., Lasslop, G., Law, B. E., Lindroth, A., Merbold, L., Montagnani, L., Moors, E. J., Papale, D., Sottocornola, M., Vaccari, F., and Williams, C.: Global patterns of land-atmosphere fluxes of carbon dioxide, latent heat, and sensible heat derived from eddy covariance, satellite, and meteorological observations, *J. Geophys. Res.-Biogeophys.*, 116, G00J07, doi:10.1029/2010JG001566, 2011.
- Kaiser, J. W., Heil, A., Andreae, M. O., Benedetti, A., Chubarova, N., Jones, L., Morcrette, J.-J., Razinger, M., Schultz, M. G., Suttie, M., and van der Werf, G. R.: Biomass burning emissions estimated with a global fire assimilation system based on observed fire radiative power, *Biogeosciences*, 9, 527–554, doi:10.5194/bg-9-527-2012, 2012.
- Keppel-Aleks, G., Wennberg, P. O., Washenfelder, R. A., Wunch, D., Schneider, T., Toon, G. C., Andres, R. J., Blavier, J.-F., Connor, B., Davis, K. J., Desai, A. R., Messerschmidt, J., Notholt, J., Roehl, C. M., Sherlock, V., Stephens, B. B., Vay, S. A., and Wofsy, S. C.: The imprint of surface fluxes and transport on variations in total column carbon dioxide, *Biogeosciences*, 9, 875–891, doi:10.5194/bg-9-875-2012, 2012.
- Kivi, R., Heikkinen, P., and Kyro, E.: TCCON data from Sodankyla, Finland, Release GGG2014R0, Tech. rep., TCCON data archive, hosted by the Carbon Dioxide Information Analysis Center, Oak Ridge National Laboratory, Oak Ridge, Tennessee, USA, doi:10.14291/tcon.ggg2014.sodankyla01.R0/1149280, 2014.
- Kulawik, S. S., Wunch, D., O'Dell, C., Frankenberg, C., Reuter, M., Oda, T., Chevallier, F., Sherlock, V., Buchwitz, M., Osterman, G., Miller, C., Wennberg, P., Griffith, D. W. T., Morino, I., Dubey, M., Deutscher, N. M., Notholt, J., Hase, F., Warneke, T., Sussmann, R., Robinson, J., Strong, K., Schneider, M., and Wolf, J.: Consistent evaluation of GOSAT, SCIAMACHY, CarbonTracker, and MACC through comparisons to TCCON, *Atmos. Meas. Tech. Discuss.*, 8, 6217–6277, doi:10.5194/amt-d-8-6217-2015, 2015.
- Lang, S. T. K., Bonavita, M., and Leutbecher, M.: On the impact of re-centring initial conditions for ensemble forecasts, *Q. J. R. Meteor. Soc.*, 141, 2571–2581, 2015.
- Le Quéré, C., Moriarty, R., Andrew, R. M., Peters, G. P., Ciais, P., Friedlingstein, P., Jones, S. D., Sitch, S., Tans, P., Arneth, A., Boden, T. A., Bopp, L., Bozec, Y., Canadell, J. G., Chini, L. P., Chevallier, F., Cosca, C. E., Harris, I., Hoppema, M., Houghton, R. A., House, J. I., Jain, A. K., Johannessen, T., Kato, E., Keeling, R. F., Kitidis, V., Klein Goldewijk, K., Koven, C., Landa, C. S., Landschützer, P., Lenton, A., Lima, I. D., Marland, G., Mathis, J. T., Metzl, N., Nojiri, Y., Olsen, A., Ono, T., Peng, S., Peters, W., Pfeil, B., Poulter, B., Raupach, M. R., Regnier, P., Rödenbeck, C., Saito, S., Salisbury, J. E., Schuster, U., Schwinger, J., Séférian, R., Segschneider, J., Steinhoff, T., Stocker, B. D., Sutton, A. J., Takahashi, T., Tilbrook, B., van der Werf, G. R., Viovy, N., Wang, Y.-P., Wanninkhof, R., Wiltshire, A., and Zeng, N.: Global carbon budget 2014, *Earth Syst. Sci. Data*, 7, 47–85, doi:10.5194/essd-7-47-2015, 2015.
- Lu, L., R.A.Pielke, Sr., G.E. Liston, W. Parton, D. Ojima, and M. Hartman: The Implementation of a two-way Interactive Atmospheric and Ecological Model and its Application to the Central United States. *Journal of Climate*, 14, 900–919, 2001.

- Massart, S., Agustí-Panareda, A., Aben, I., Butz, A., Chevallier, F., Crevoisier, C., Engelen, R., Frankenberg, C., and Hasekamp, O.: Assimilation of atmospheric methane products into the MACC-II system: from SCIAMACHY to TANSO and IASI, *Atmos. Chem. Phys.*, 14, 6139–6158, doi:10.5194/acp-14-6139-2014, 2014.
- Massart, S., Agustí-Panareda, A., Heymann, J., Buchwitz, M., Chevallier, F., Reuter, M., Hilker, M., Burrows, J. P., Hase, F., Desmet, F., Feist, D. G., and Kivi, R.: Ability of the 4-D-Var analysis of the GOSAT BESD XCO<sub>2</sub> retrievals to characterize atmospheric CO<sub>2</sub> at large and synoptic scales, *Atmos. Chem. Phys.*, 16, 1653–1671, doi:10.5194/acp-16-1653-2016, 2016.
- Messerschmidt, J., N. Parazoo, D. Wunch, N.M. Deutscher, C. Roehl, T. Warneke and P.O. Wennberg: Evaluation of seasonal atmosphere-biosphere exchange estimations with TCCON measurements, *Atmospheric Chemistry and Physics*, 13, 5103–5115, doi:10.5194/acp-13-5103-2013, 2013.
- Morcrette, J.-J., J.-J., Boucher, O., Jones, L., Salmond, D., Bechtold, P., Beljaars, A., Benedetti, A., Bonet, A., Kaiser, J., Razinger, M., Schulz, M., Serrar, S., Simmons, A., Sofiev, M., Suttie, M., Tompkins, A., and Untch, A.: Aerosol analysis and forecast in the European Centre for Medium-Range Weather Forecasts Integrated Forecast System: Forward modeling, *J. Geophys. Res.*, 114, D06206, doi:10.1029/2008JD011235, 2009.
- Moreira, D. S., Freitas, S. R., Bonatti, J. P., Mercado, L. M., Rosário, N. M. É., Longo, K. M., Miller, J. B., Gloor, M., Gatti, L. V.: Coupling between the JULES land-surface scheme and the CCATT-BRAMS atmospheric chemistry model (JULES-CCATT-BRAMS1.0): applications to numerical weather forecasting and the CO<sub>2</sub> budget in South America, *Geoscientific Model Development*, 6, 1243–1259, doi:10.5194/gmd-6-1243-2013, 2013.
- Nassar, R. and Jones, D. B. A. and Suntharalingam, P. and Chen, J. M. and Andres, R. J. and Wecht, K. J. and Yantosca, R. M. and Kulawik, S. S., Bowman and K. W. and Worden, J. R. and Machida, T. and Matsueda, H. (2010): Modeling global atmospheric CO<sub>2</sub> with improved emission inventories and CO<sub>2</sub> production from the oxidation of other carbon species, *Geosci. Model Dev.*, 3, 689–716, doi:10.5194/gmd-3-689-2010, 2010.
- Cooperative Global Atmospheric Data Integration Project; Multi-laboratory compilation of atmospheric carbon dioxide data for the period 1968–2014; *obspack\_co2\_1\_GLOBALVIEWplus\_v1.0\_2015-07-30*; NOAA Earth System Research Laboratory, Global Monitoring Division. doi: 10.15138/G3RP42, <http://dx.doi.org/10.15138/G3RP42>
- Olson, J.: Global Ecosystems Framework: Definitions, U.S. Geological Survey, Sioux Falls, SD, USA, 37 pp., 1994a.
- Olson, J.: Global Ecosystems Framework: Translation strategy, U.S. Geological Survey, Sioux Falls, SD, USA, 39 p., 1994b.
- Palmer, T., Buizza, R., Doblas Reyes, F., Jung, T., Leutbech, M., Shutts, G., Steinheimer, M., and Weisheimer, A.: Stochastic parametrization and model uncertainty, Technical Memorandum 598, ECMWF, ECMWF, Shinfield Park, Reading, RG2 9AX, UK, 2009.
- Peters, W., Jacobson, A., Sweeney, C., Andrews, A., Conway, T., Masarie, K., Miller, J., Bruhwiler, L., Petron, G., Hirsch, A., Worthy, D., van der Werf, G., Randerson, J., Wennberg, P., Krol, M., and Tans, P.: An atmospheric perspective on North American carbon dioxide exchange: CarbonTracker, *P. Natl. Acad. Sci.*, 104, 18925–18930, doi:10.1073/pnas.0708986104, 2007.
- Peylin, P., Law, R. M., Gurney, K. R., Chevallier, F., Jacobson, A. R., Maki, T., Niwa, Y., Patra, P. K., Peters, W., Rayner, P. J., Rödenbeck, C., van der Laan-Luijkx, I. T., and Zhang, X.: Global atmospheric carbon budget: results from an ensemble of atmospheric CO<sub>2</sub> inversions, *Biogeosciences*, 10, 6699–6720, doi:10.5194/bg-10-6699-2013, 2013.
- Polavarapu, S.M., M. Neish, M. Tanguay, C. Girard, J. de Grandpré, S. Gravel, K. Semeniuk, and D. Chan (2015): Adapting a weather forecast model for greenhouse gas simulation, AGU Fall Meeting, San Francisco, 15–18 December 2015, Poster A31B-0037.
- Rayner, P., Scholze, M., Knorr, W., Kaminski, T., Giering, R., and Widmann, H.: Two decades of terrestrial carbon fluxes from a carbon cycle data assimilation system (CCDAS), *Global Biogeochem. Cy.*, 19, GB2026, doi:10.1029/2004gb002254, 2005.
- Rayner, P., Koffi, E., Scholze, M., Kaminski, T., and Dufresne, J.-L.: Constraining predictions of the carbon cycle using data, *P. T. R. Soc. A*, 369, 1955–1966, doi:10.1098/rsta.2010.0378, 2011.
- Rödenbeck, C., Houweling, S., Gloor, M., and Heimann, M.: CO<sub>2</sub> flux history 1982–2001 inferred from atmospheric data using a global inversion of atmospheric transport, *Atmos. Chem. Phys.*, 3, 1919–1964, doi:10.5194/acp-3-1919-2003, 2003.
- Schaefer, K., A.S. Denning, N. Suits, J. Kaduk, I. Baker, S. Losd, and L. Prihodko (2002): Effect of climate on inter-annual variability of terrestrial CO<sub>2</sub> fluxes, *Global Biogeochemical Cycles*, 16, 2002.
- Schepers, D., S. Guerlet, A. Butz, J. Landgraf, C. Frankenberg, O. Hasekamp and J.-F. Blavier, N.M. Deutscher, D.W.T. Griffith and F. Hase, E. Kyro, I. Morino, V. Sherlock, R. Sussmann, and I. Aben: Methane retrievals from Greenhouse Gases Observing Satellite (GOSAT) shortwave infrared measurements: Performance comparison of proxy and physics retrieval algorithms, *Journal of Geophysical Research*, 117, D10307, doi:10.1029/2012JD017549, 2012.
- Scholze, M., Kaminski, T., Rayner, P., Knorr, W., and Giering, R.: Propagating uncertainty through prognostic carbon cycle data assimilation system simulations, *J. Geophys. Res.*, 112, D17305, doi:10.1029/2007JD008642, 2007.
- Sweeney, C., A. Karion, S. Wolter, T. Newberger, D. Guenther, J. A. Higgs and A. E. Andrews, P. M. Lang, D. Neff, E. Dlugokencky, J. B. Miller and S. A. Montzka, B. R. Miller, K. A. Masarie, S. C. Biraud, P. C. Novelli, M. Crotwell, A. M. Crotwell, K. Thoning, and P. P. Tans: Seasonal climatology of CO<sub>2</sub> across North America from aircraft measurements in the NOAA/ESRL Global Greenhouse Gas Reference Network, *Journal of Geophysical Research: Atmospheres*, 120, 10, doi:10.1002/2014JD022591, 2015.
- Takahashi, T., Sutherland, S., Wanninkhof, R., Sweeney, C., Feely, R., Chipman, D., Hales, B., Friederich, G., Chavez, F., Watson, A., Bakker, D., Schuster, U., Metz, N., Yoshikawa-Inoue, H., Ishii, M., Midorikawa, T., Nojiri, Y., Sabine, C., Olafsson, J., Arnarson, T., Tilbrook, B., Johannessen, T., Olsen, A., Bellerby, R., Krtzinger, A., Steinhoff, T., Hoppema, M., de Baar, H., Wong, C., Delille, B., and Bates, N. R.: Climatological mean and decadal changes in surface ocean pCO<sub>2</sub>, and net sea-air CO<sub>2</sub> flux over the global oceans, *Deep-Sea Res. II*, 56, 554–577, 2009.
- Thoning, K., Kitzis, D., and Crotwell, A.: Atmospheric Carbon Dioxide Dry Air Mole Fractions from quasi-continuous measure-

- ments at Barrow, Alaska; Mauna Loa, Hawaii; American Samoa; and South Pole, 1973–2011, Version: 2012-05-07, Tech. Rep., NOAA, available at: [ftp://ftp.cmdl.noaa.gov/data/greenhouse\\_gases/co2/in-situ/](ftp://ftp.cmdl.noaa.gov/data/greenhouse_gases/co2/in-situ/) (last access: 18 December 2015), 2012.
- Trémolet, Y.: Accounting for an imperfect model in 4D-Var, Q. J. R. Meteor. Soc., 132, 2483–2504, 2006.
- Trémolet, Y.: Model-error estimation in 4D-Var, Q. J. R. Meteor. Soc., 133, 1267–1280, doi:10.1002/qj.94, 2007.
- Vitart, F.: Evolution of ECMWF sub-seasonal forecast skill scores over the past 10 years, Technical Memorandum 694, ECMWF, available at: [www.ecmwf.int/en/elibrary/miscellaneous/12932-evolution-ecmwf-sub-seasonal-forecast-skill-scores-over-past-10](http://www.ecmwf.int/en/elibrary/miscellaneous/12932-evolution-ecmwf-sub-seasonal-forecast-skill-scores-over-past-10) (last access: 5 January 2016), 2013.
- Vitart, F.: Evolution of ECMWF sub-seasonal forecast skill scores, Q. J. R. Meteor. Soc., 140, 1889–1899, 2014.
- Vitart, F., Buizza, R., Balmaseda, M. A., Balsamo, G., Bidlot, J.-R., Bonet, A., Fuentes, M., Hofstadler, A., Molteni, F., and Palmer, T.: The new VAREPS-monthly forecasting system: a first step towards seamless prediction, Q. J. R. Meteor. Soc., 134, 1789–1799, 2008.
- Wennberg, P. O., Wunch, D., Roehl, C., Blavier, J.-F., Toon, G. C., Allen, N., Dowell, P., Teske, K., Martin, C., and Martin, J.: TCCON data from Lamont, Oklahoma, USA, Release GGG2014R0, Tech. rep., TCCON data archive, hosted by the Carbon Dioxide Information Analysis Center, Oak Ridge National Laboratory, Oak Ridge, Tennessee, USA, doi:10.14291/tcon.ggg2014.sodankyla01.R0/1149280, 2014.
- Wunch, D., Toon, G. C., Blavier, J.-F. L., Washenfelder, R. A., Notholt, J., Connor, B., Griffith, D. W. T., Sherlock, V., and Wennberg, P. O.: The total carbon column observing network, P. T. R. Soc. A, 369, 2087–2112, doi:10.1098/rsta.2010.0240, 2011.

**Table 1.** Percentage of land grid points at model resolution TL255 ( $\sim 80$  km) for each dominant vegetation type, i.e. more than half of the grid point is covered by that vegetation type. A land grid point is defined by a land sea mask value greater than 0.5.

Vegetation Code	Vegetation type	Percentage of land points
1	Crops, Mixed Farming	9.9
2	Short Grass	7.6
7	Tall Grass	6.3
9	Tundra	6.3
10	Irrigated Crops	2.2
11	Semidesert	13.5
13	Bogs and Marshes	0.8
16	Evergreen Shrubs	0.5
17	Deciduous Shrubs	2.4
3	Evergreen Needle leaf Trees	5.7
4	Deciduous Needle leaf Trees	2.4
5	Deciduous Broadleaf Trees	4.0
6	Evergreen Broadleaf Trees	12.1
18	Mixed Forest/woodland	3.3
19	Interrupted Forest	9.5
21	Tropical Savanna (new type)	4.8
–	Remaining land points without vegetation	8.7

**Table 2.** List of simulations with the same transport and different CO<sub>2</sub> surface fluxes.

Experiment name	CO <sub>2</sub> surface fluxes
CTRL	Biogenic fluxes from CTESSEL (Boussetta et al., 2013), biomass burning fluxes from GFAS (Kaiser et al., 2012), ocean fluxes from Takahashi et al. (2009), and EDGAR v4.2 anthropogenic fluxes (Janssens-Maenhout et al., 2012)
OPT	MACC-13R1 optimised fluxes (Chevallier et al., 2010) for 2010
OPT-CLIM	MACC-13R1 optimised flux climatology (2004–2013)
BFAS	Same fluxes as CTRL including BFAS

**Table 3.** List of TCCON stations used in Fig. 10 ordered by latitude from North to South.

Site	Latitude [degrees]	Longitude [degrees]	Altitude [m a.s.l]	Reference
Sodankylä	67.37	26.63	190.0	Kivi et al. (2014)
Białystok	53.23	23.02	160.0	Deutscher et al. (2014)
Lamont	36.60	−97.49	320.0	Wennberg et al. (2014)
Wollongong	−34.41	150.88	30.0	Griffith et al. (2014)

**Table 4.** Correlation coefficient of different forecast (FC) experiments (see Table 2) with observations at three NOAA/ESRL tall towers for daily mean dry molar fraction of atmospheric CO<sub>2</sub> in March 2010. The dash symbol means the correlation is not significant.

NOAA/ESRL Tower site (ID)	Latitude, Longitude, Altitude	Sampling level [m]	BFAS FC	CTRL FC	OPT FC	OPT-CLIM FC
Park Falls, Wisconsin (LEF)	45.95° N, 90.27° W, 472 m	30	0.843	0.338	0.794	0.797
		122	0.931	0.508	0.893	0.883
		396	0.919	–	0.875	0.881
West Branch, Iowa (WBI)	41.72° N, 91.35° W, 242 m	31	0.748	0.496	0.590	0.590
		99	0.833	0.436	0.767	0.720
		379	0.851	0.356	0.887	0.876
Argyle, Maine (AMT)	45.03° N, 68.68° W, 50 m	12	0.857	0.839	0.808	0.893
		30	0.875	0.835	0.816	0.938
		107	0.861	0.668	0.816	0.927



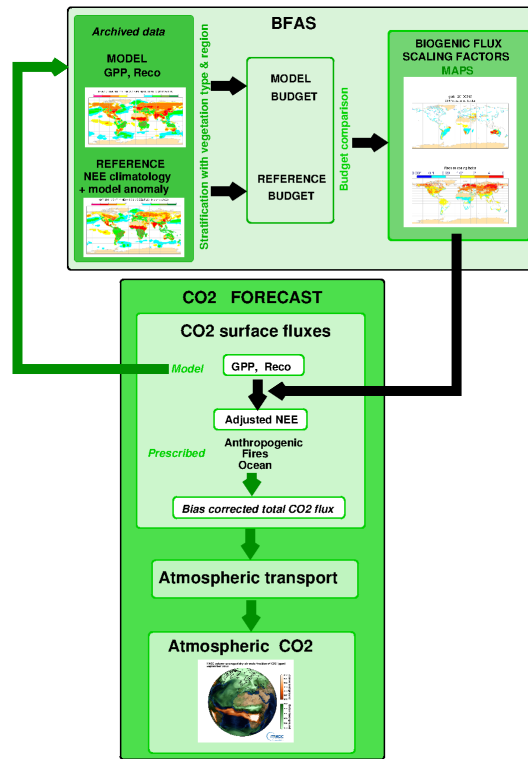


**Figure 1.** Schematic showing how BFAS fits in the atmospheric CO<sub>2</sub> forecasting system. BFAS is called before each forecast to compute the scaling factors for the model NEE (i.e.  $GPP + R_{eco}$ ) based on the past archived forecasts. The maps of the scaling factors are then passed to the model which applies the adjustment to the output biogenic CO<sub>2</sub> fluxes from the land surface model. After combining the adjusted NEE fields with the other prescribed CO<sub>2</sub> fluxes, the resulting bias corrected fluxes are passed to the transport model to produce the atmospheric CO<sub>2</sub> forecast.

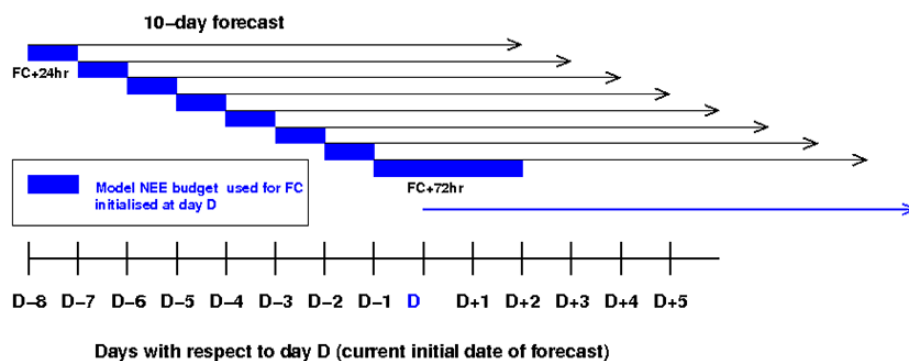


**Figure 2.** Schematic to illustrate how the 10-day NEE budget from the model is computed in BFAS for the forecast at day  $D$  by retrieving the past forecasts of accumulated NEE. Note that the retrieved NEE (computed by adding GPP and  $R_{\text{eco}}$ ) has not been corrected by BFAS. The computation uses a set of 7 previous 1-day forecasts (initialised at  $D-8$ ,  $D-7$ ,  $D-6$ , ..., until  $D-2$ ) together with the latest 3-day forecast from the previous day (i.e.  $D-1$ ) as shown by the blue boxes.

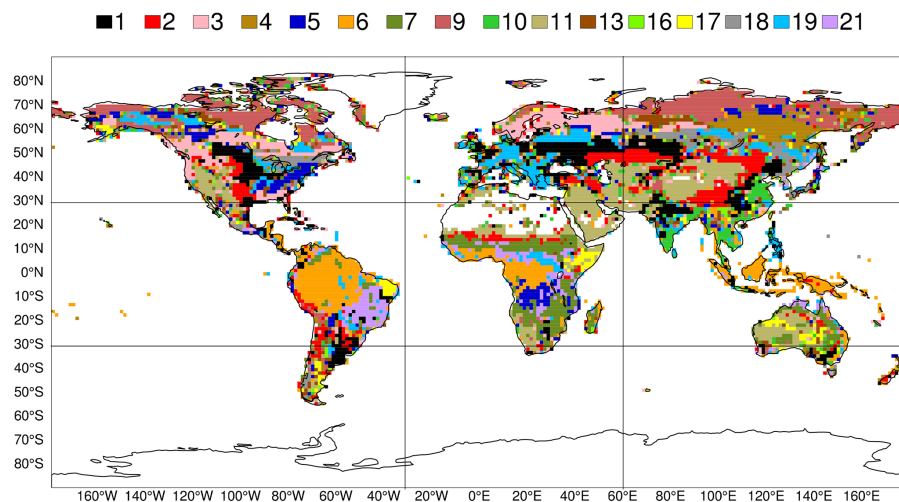


**Figure 3.** Dominant vegetation types based on the BATS classification used in the IFS and extended to include the tropical savanna subtype (in purple, as defined by the Olson (1994a) classification) within the interrupted forest type (in light blue). The vegetation type codes are described in Table 1. The nine regions used in the computation of the NEE budget are delimited by the black lines.

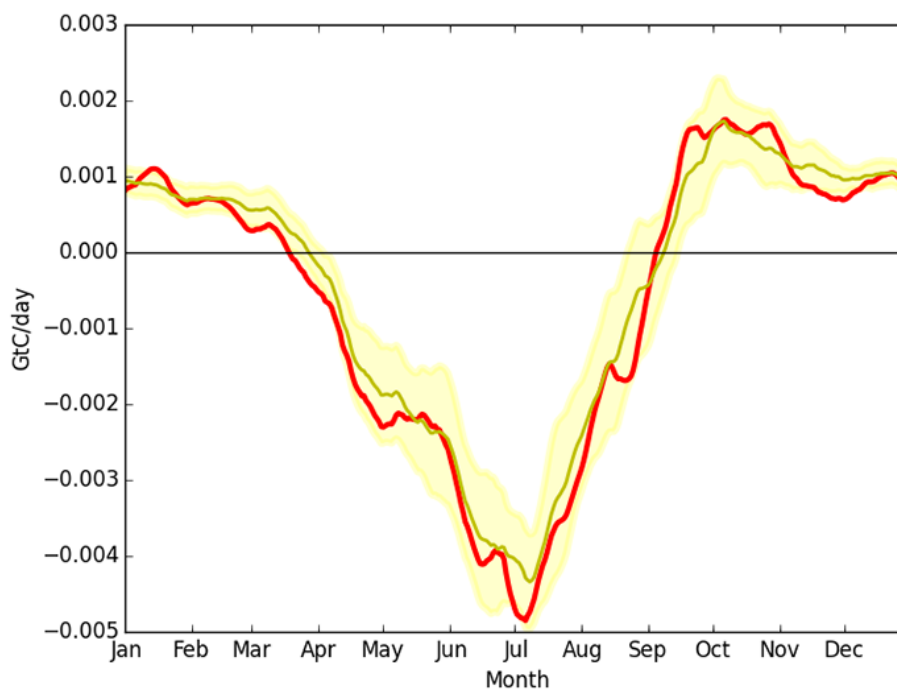


**Figure 4.** Time series of 10-day mean NEE budget [GtC/day] associated with the crop vegetation type in North America from the MACC-13R1 optimised flux data set in 2010 (red line) compared to its climatology (2004–2013) (yellow line). The yellow shading represents the standard deviation of the optimised flux budget (for the same period) used to compute the inter-annual variability adjustment applied to the reference climatology. Positive/negative values correspond to a source/sink of CO<sub>2</sub>.

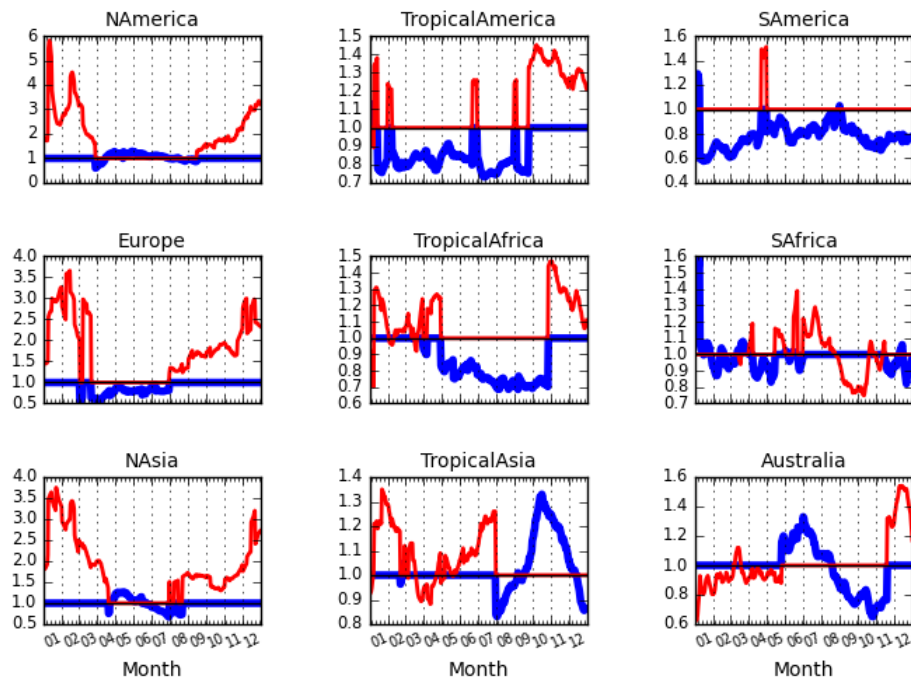


**Figure 5.** Time series of GPP and  $R_{eco}$  flux scaling factors in blue and red lines respectively for the crop vegetation type in 2010 in the different regions (see map in Fig. 3 depicting the extent of the crops within each region).

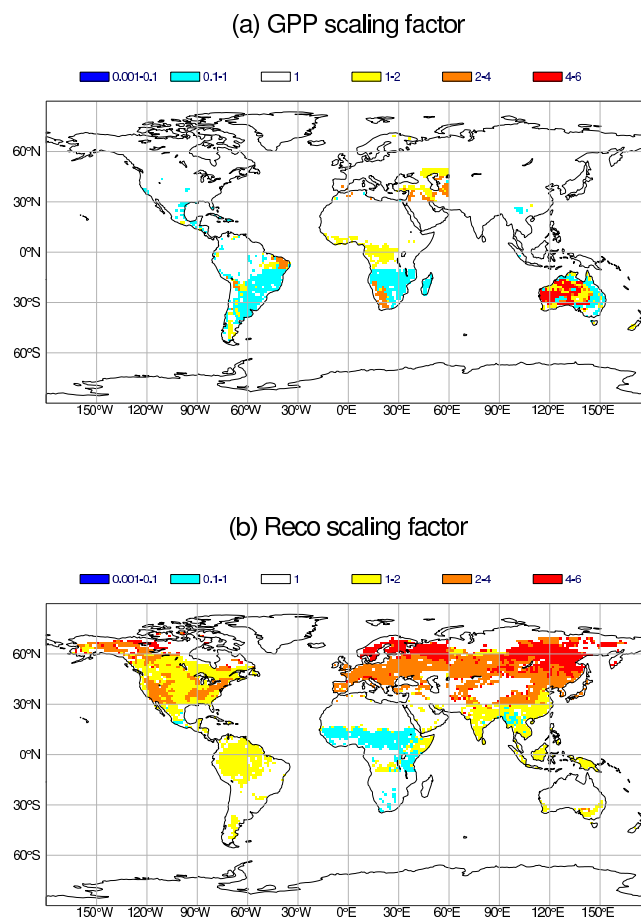


**Figure 6.** Map of scaling factors for (a) GPP and (b)  $R_{\text{eco}}$  on 15 March 2010.

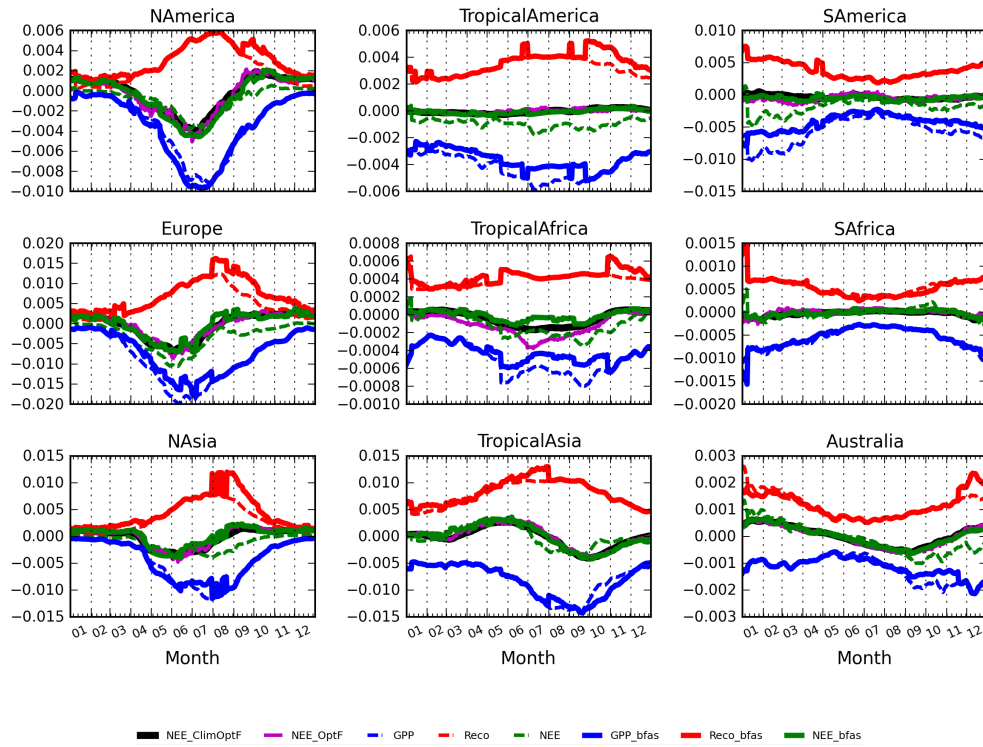


**Figure 7.** Time series of GPP (in blue),  $R_{\text{eco}}$  (in red) and NEE (in green) daily budget [GtC/day] before and after the flux adjustment (see dashed lines and solid lines respectively) for crops in 2010 in the different regions. The reference budget provided by the climatology of MACC-13R1 optimised fluxes (2004–2013) and the MACC-13R1 optimised fluxes for 2010 are depicted by the black and magenta lines respectively. Positive/negative values correspond to a source/sink of CO<sub>2</sub>.



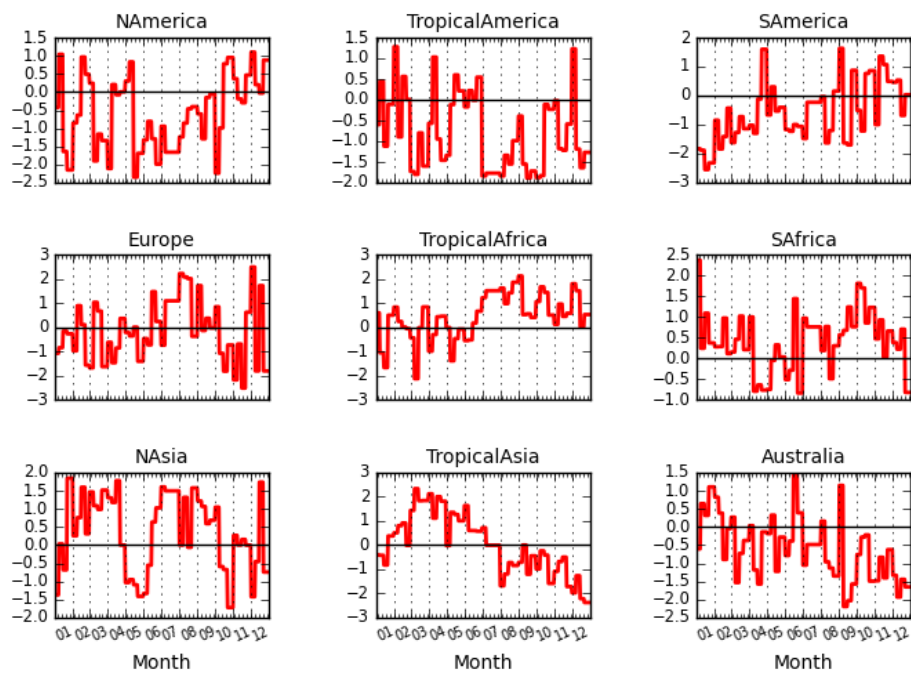


**Figure 8.** Time series of the standardised anomaly of the modelled NEE budget ( $\gamma$  in Eq. 3) for crops in 2010 in the different regions. Positive values indicate larger/smaller CO<sub>2</sub> sources/sinks than normal based on the mean climatological budget; whereas negative values correspond to smaller/larger CO<sub>2</sub> sources/sinks than normal.

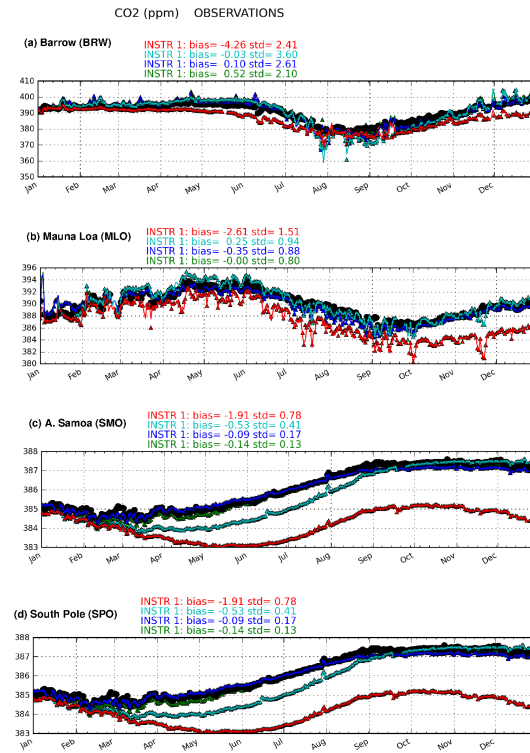


**Figure 9.** Daily mean atmospheric CO<sub>2</sub> dry molar fraction [ppm] from NOAA/ESRL continuous baseline stations (black circles) at **(a)** Barrow, Alaska, USA (71.32° N, 156.61° W), **(b)** Mauna Loa, Hawaii, US (19.54° N, 155.58° W), **(c)** Tutuila, American Samoa, USA (14.25° S, 170.56° W), **(d)** South Pole, Antarctica (89.98° S, 24.8° W) and the different forecast experiments: BFAS (cyan), CTRL (red), OPT (green) and OPT-CLIM (blue). See Table 2 for a description of the different experiments. The mean (bias) and standard deviation (SD) of the model errors are shown at the top of each panel.

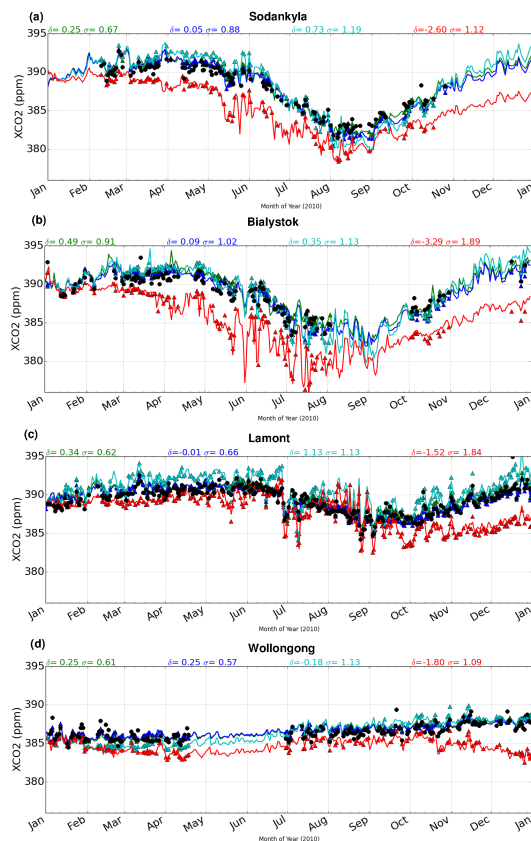


**Figure 10.** Daily mean atmospheric CO<sub>2</sub> column-average dry molar fraction [ppm] observed at four TCCON stations (see Table 3) as shown by the black circles, and simulated by the different forecast experiments: BFAS (cyan), CTRL (red), OPT (green) and OPT-CLIM (blue). See Table 2 for a description of the different experiments. The mean ( $\delta$ ) and standard deviation ( $\sigma$ ) of the model errors are shown at the top of each panel.

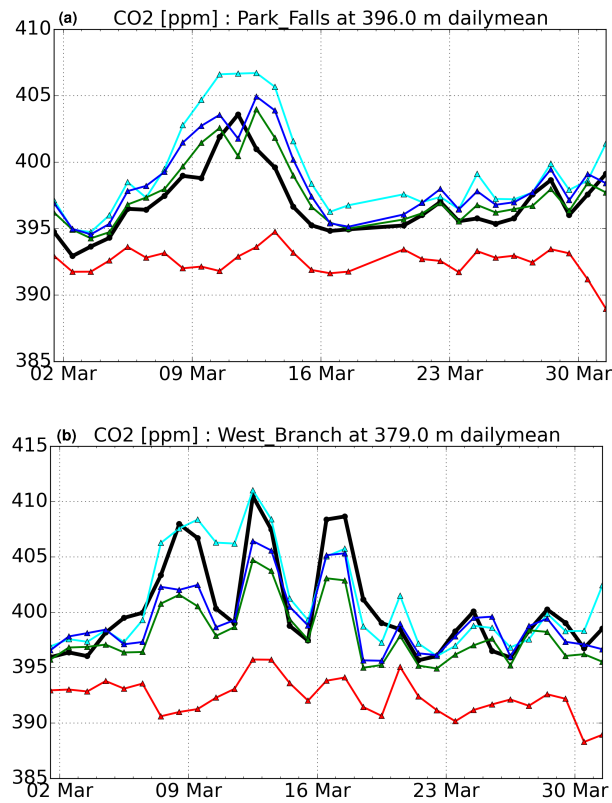


**Figure 11.** Daily mean atmospheric CO<sub>2</sub> dry molar fraction [ppm] in March 2010 from NOAA/ESRL tall towers (black circles) at **(a)** Park Falls (Wisconsin, USA, 45.95° N, 90.27° W) and **(b)** West Branch (Iowa, USA, 41.72° N, 91.35° W) and the different forecast experiments: BFAS (cyan), CTRL (red), OPT (green) and OPT-CLIM (blue) (see Table 2 for a description of the different experiments).

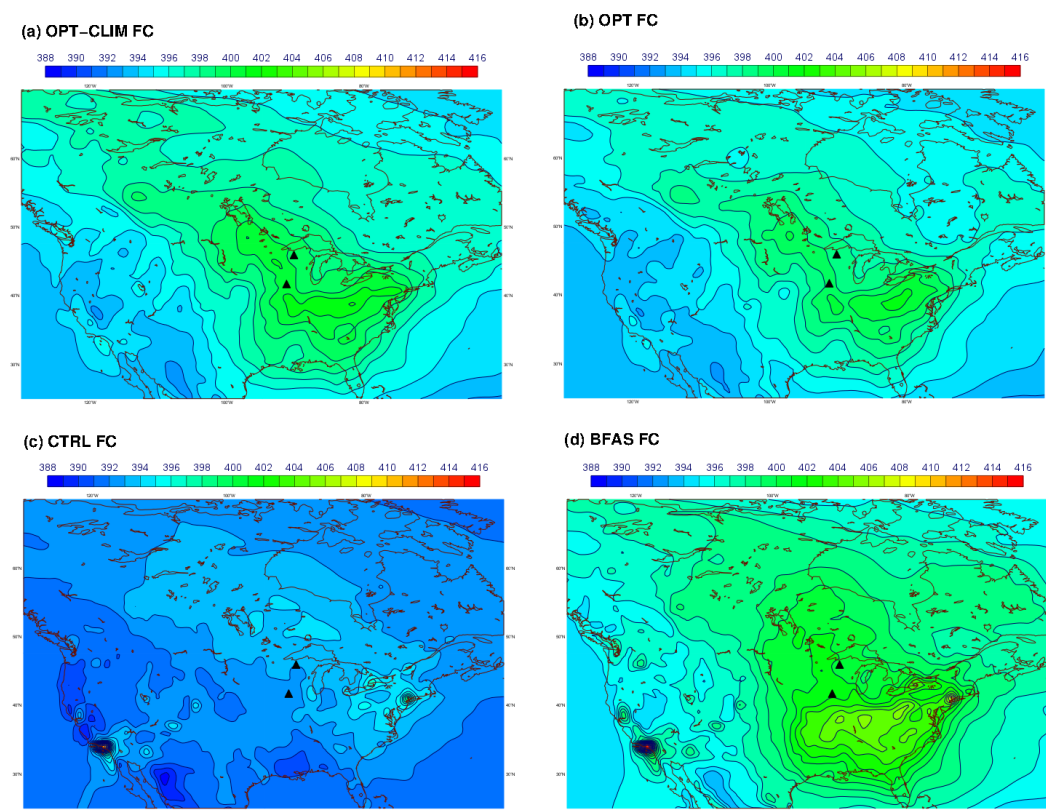


**Figure 12.** Monthly mean atmospheric CO<sub>2</sub> dry molar fraction [ppm] at the model level approximately corresponding to the highest sampling height of the Park Falls and West Branch NOAA/ESRL tall towers (see black triangles) in March 2010 from (a) OPT-CLIM, (b) OPT, (c) CTRL and (d) BFAS experiments (see Table 2 for a description of the different experiments).

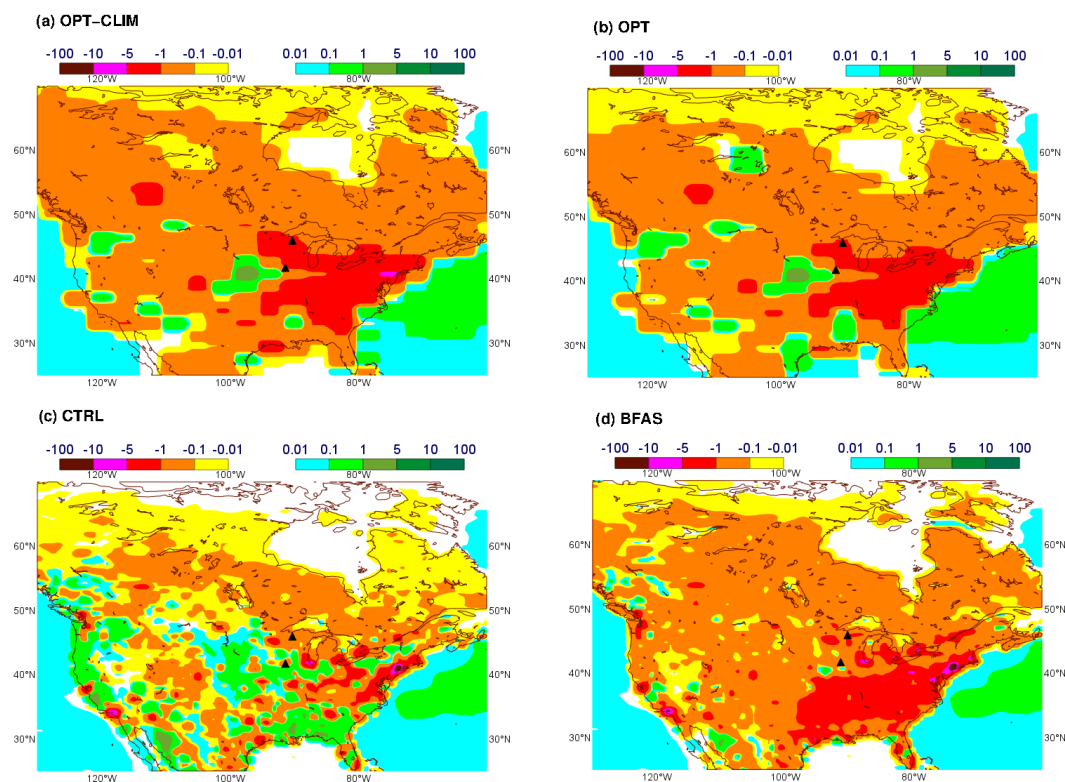


**Figure 13.** Monthly mean total CO<sub>2</sub> flux [ $\mu\text{mol m}^{-2} \text{s}^{-1}$ ] in March 2010 from (a) OPT-CLIM, (b) OPT, (c) CTRL and (d) BFAS experiments (see Table 2 for a description of the different experiments). The black triangles depict the location of the NOAA/ESRL tall towers plotted in Fig. 11.